

Morphological and Genetic Variation Among Populations of the Fiddler Crab *Minuca burgersi* (Holthuis, 1967) (Crustacea: Brachyura: Ocypodidae) from Shores of the Caribbean Basin and Western South Atlantic Ocean

C. L. Thurman¹, R. E. Alber¹, M. J. Hopkins², and Hsi-Te Shih^{3*}

¹Department of Biology, University of Northern Iowa, 1227 West 27th St., Cedar Falls, IA 50614-0421, USA. E-mail: thurman@uni.edu (Thurman); meierreid@gmail.com (Alber)

²Division of Paleontology, American Museum of Natural History, Central Park West at 79th Street, New York, NY 10024-5192, USA. E-mail: mhopkins@amnh.org (Hopkins)

³Department of Life Science and Research Center for Global Change Biology, National Chung Hsing University, Taichung 402, Taiwan.

*Correspondence: E-mail: htshih@dragon.nchu.edu.tw (Shih)

Received 14 September 2020 / Accepted 10 February 2021 / Published 29 April 2021

Communicated by Benny K.K. Chan

For this study, in addition to museum vouchers, 1437 specimens of *Minuca burgersi* (Holthuis, 1967) were collected from crab colonies at 105 locations in the western Atlantic Ocean to examine diversity in a species with a large geographic range. Both allometric and geometric morphometry were coupled with the molecular analysis of DNA to give a broader perspective of intraspecific variability in this species. A total of 1153 specimens from the Caribbean Sea and the Atlantic coast of South America demonstrated that *M. burgersi* from both regions are very similar in their pattern of growth. The average carapace width (CW) for Caribbean is larger than the average for South American males and females. However, size distribution based on CW is unimodal in Caribbean and bimodal in South American populations. The carapace length-width ratio is about 0.68 in females and 0.66 in males. South American males express asymmetric elongation of the cheliped in smaller CW intervals than Caribbean males. In a sample of 259 females, carapace shape is distinct between South American and Caribbean populations. Caribbean populations have less swelling in the branchial regions than South American populations. The swelling correlates primarily with geographic region and to a lesser degree with substrate and salinity. Molecular data from the 16S rDNA and cytochrome c oxidase subunit I (COI) reveal three clades within *Minuca burgersi*. Two clades are distributed in the Caribbean and the third in eastern South America. The timing of divergence between Caribbean and South American clades is coincident with an increased rate of water and sediment outflow from the Amazon as inferred from the geologic record. Current patterns and associated gene flow within the Caribbean were subsequently influenced by the closing of the Isthmus of Panama. We speculate that various populations may employ different larval dispersion mechanisms resulting in genetic heterogeneity. Consequently, there is considerable biological divergence among populations of *M. burgersi* in the Caribbean and South America.

Key words: Fiddler crab, Biogeography, Diversity, Morphology, Allometry, Geometric morphometrics, 16S rDNA, Cytochrome c oxidase subunit I (COI), Molecular phylogeny.

BACKGROUND

Very few species are known from a single locality. Instead species are comprised of spatially distributed populations that may encounter a wide range of environments. Thus, it might be expected that populations separated by a great distance are more likely to express phenotypic divergence due to substantial physical heterogeneity of habitats across the range. However, the extent to which environmental heterogeneity promotes phenotypic variation among populations depends on how strongly the phenotype is linked to the underlying genotypes as well as patterns of gene flow (Wright 1930; Levins 1968; Endler 1977). For example, free gene flow among populations will promote genotypic uniformity (Grantham et al. 2003; Kelly and Palumbi 2010). In that case, phenotype diversity would result largely from varied epigenetic regulation. On the other hand, if there are environmental or physical barriers preventing dispersal and gene transport by propagules, the resulting isolation could lead to local inbreeding and/or selection, and promote the appearance of several populations with distinct phenotypes and/or genotypes. In the latter case, the spatial pattern of genotype/phenotype distributions could be described as a “patchwork” (Levins 1968), where measures of variation are expected to be greater between populations than within populations. Distinct variation among populations would support the concept that a species is a complex of divergent but geographically structured populations. Over longer timescales, the persistence of morphological and genetic divergence between proximal and remote populations could result in speciation (Endler 1977). To study these processes, it is necessary to quantify broad-spectrum patterns of genotypic and phenotypic variables in taxa with both large geographic ranges and varied dispersal potential.

A model marine species for exploring the nuances of intraspecific variation in widely dispersed populations is the semi-terrestrial crab. Fiddler crabs are semi-terrestrial decapod crustaceans inhabiting temperate and tropical coasts around the world (Crane 1975). Adults live at one location where they produce ova and planktonic larvae. The planktonic phase temporarily resides in bays and coastal waters where they mature (Hyman 1922). After release, the zoeae are dispersed by tides and ocean currents. Eventually zoeae undergo metamorphosis into the megalopal stage and settle on an appropriate shore (Behum et al. 2005; Brodie et al. 2005). During the adult phase, these crabs select habitats ranging from sand to mud washed by waters of varying salinities. Along the coast of the western Atlantic Ocean, there are 21 described species of fiddler crabs (Beinlich

and von Hagen 2006). Among these, five species have distribution ranges from southern Brazil to Mexico and Florida (Thurman et al. 2013, Rosenberg 2020). One is *Minuca burgersi* (Holthuis, 1967), which is distributed from Dania Beach, Florida to Fazenda, Santa Catarina, Brazil (Thurman et al. 2013). Across 6700 km (4200 mi) of latitude, *M. burgersi* live in different habitats such as sand flats, isolated mangroves, rivers, and lagoons, and could potentially express morphological and genetic variation.

Taxonomic History

Minuca burgersi and other closely related species have a complex and intertwined taxonomic history due to past sorting and re-sorting of species and subgenera. In 1880, J. S. Kingsley (1880)? reduced the number of fiddler crab taxa in an attempt to arrive at the “true number of species.” In this study, the species *M. burgersi*, previously known as *Gelasimus affinis* Streets, 1872, was classified under “*Gelasimus vocator* v. *Martin*,” along with eleven other previously distinct species. After examining crabs from Suriname (Dutch Guiana), Holthuis (1959) resurrected *C. vocator* Herbst, 1804, as a distinct species. Then in 1967, Holthuis presented a short description of *Uca burgersi* based on holotype (Rijks Museum no. 23012) and paratype (US National Museum no. 121099) material collected from Westpunt, Curaçao, Netherlands Antilles. Specimens for the description ranged from southern Florida, eastern Mexico, through the Caribbean to the Netherlands Antilles.

Almost immediately, Chase and Hobbs (1969) published a more elaborated description of *U. burgersi* based on 81 specimens captured on the Leeward Caribbean island of Dominica. Describing the ecological habitat of the species, they seemed to find it primarily on riverbanks or in areas of low salinity with no clear connection to the Caribbean. Geographically, the authors reported *U. burgersi* only from Caribbean islands. Meanwhile in Brazil, Coelho (1972) presented an abstract in which he gave a preliminary description of a new species *Uca panema* Coelho, 1972. The author noted that *Uca mordax* (Smith 1970) is absent from the rivers in the states of Pernambuco and Pariaba. Instead, a different, undescribed species was present in low salinity, supra-littoral environments. Coelho referred to the new species as *Uca panema* in honor of the first fiddler crab species described for Brazil by Marcgrave (1648: 185, as “Ciecie Panema”).

In 1975, Crane published her monographic tome revising and organizing the genus *Uca* into a number of subgenera, species, and subspecies. She placed *U. burgersi* into the *Minuca* subgenus with other species

including *U. vocator*, *U. mordax*, *U. minax*, and *U. rapax*. At that time, she reported *U. burgersi* to range from Florida, the Yucatan, Belize, Guatemala, Panama, Venezuela and throughout the Caribbean islands. In addition, for the first time, she added specimens from Fortaleza (USNM 138509), Rio de Janeiro (USNM 136511), and São Sebastião (USNM 1136004, 138510) in Brazil. It appears that Crane's recognition of *U. burgersi* in Brazil suppressed a complete description for *Uca panema* by Coelho, and *U. panema* has been treated as a junior synonym of *U. burgersi* (Beinlich and von Hagen 2006; Shih et al. 2016). In 1996, Melo published a catalog of crabs from littoral habitats in Brazil. By his interpretation, *U. burgersi* is distributed from Florida and the Gulf of Mexico to northern South America. He considered the species to be absent from Guyana, Suriname and French Guiana as well as Brazilian areas

north of the Amazon estuary (Melo 1996). Along the Brazil coast, he reported it from San Luis to Cabo Frio near Rio de Janeiro. Based on new molecular evidence, Shih et al. (2016) reorganized fiddler crab species into 11 genera, elevating previous subgeneric classifications. The result is that the species is named *Minuca burgersi* (Holthuis, 1967).

Conspectus

Minuca burgersi occurs in the western Atlantic from southern Florida to southern Brazil. Fieldwork in recent years (Thurman et al. 2010 2013 2018) failed to uncover *M. burgersi* along the 1,650 km (1025 mi) coast of northeast South America between the Amazon and Orinoco rivers (Fig. 1). However, the species was found on Trinidad and Barbados in the southeastern

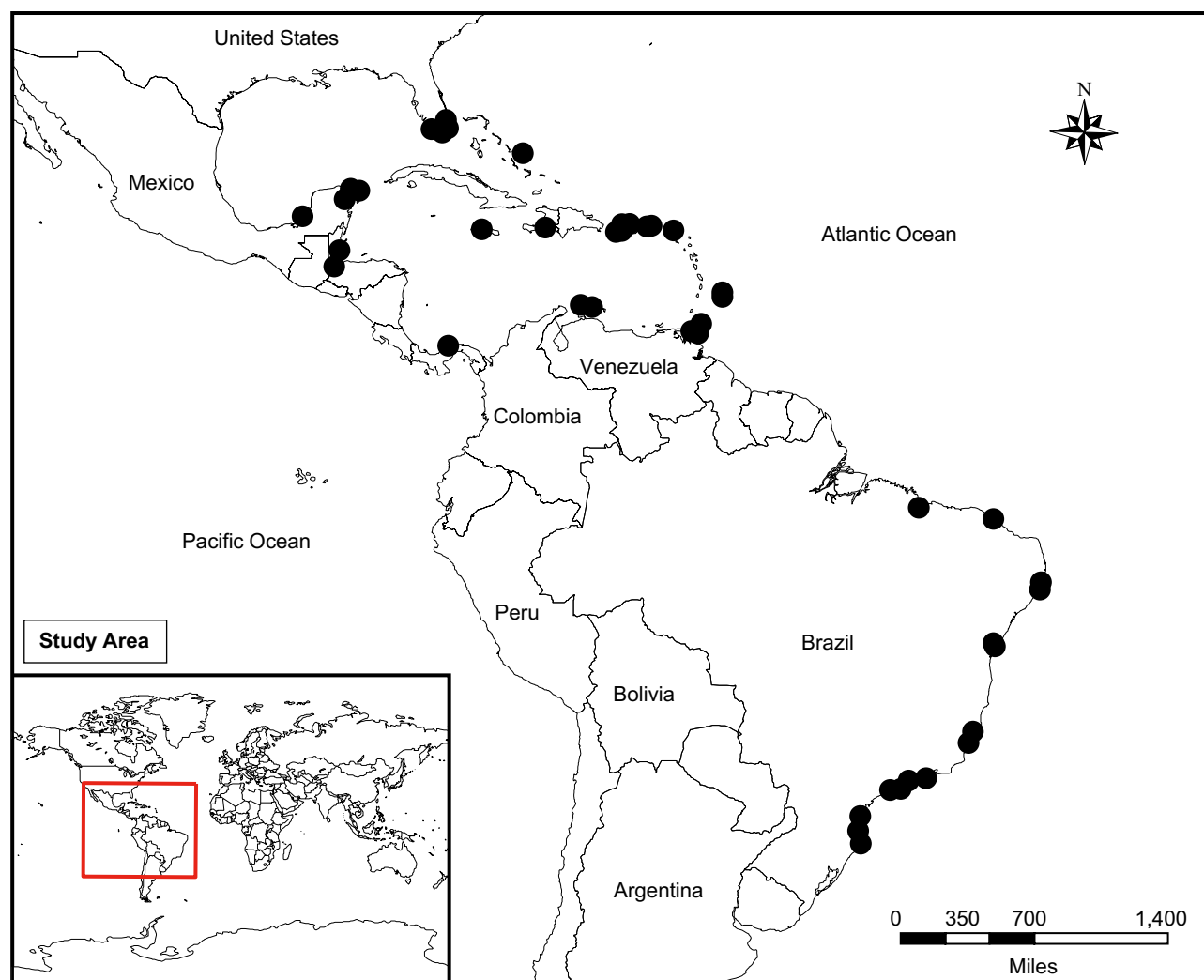


Fig. 1. Approximate location (●) of 105 sample sites for *Minuca burgersi* in the USA, Mexico, Caribbean and eastern South America. At some dots cover several locations. See table S1a and S1b for exact locations.

Caribbean. It is also known to occur along the coast of northern Brazil, south of the state of Pará (Universidade do São Paulo Zoological Museum (MZUSP) specimen #12313). Since the nearshore Guyana current flows to the northwest, the low-salinity muddy river effluence may limit the larvae of South American *M. burgersi* from accessing the southern Caribbean. Thus, freshwater outflow, from either the Amazon or Orinoco river, and the lack of sandy substrates along the coast is presumed to pose a geographic barrier preventing the settling of larvae and development of *M. burgersi* colonies between the Caribbean and Brazil.

Previous studies examined *M. burgersi* populations from restricted locations in the Caribbean and South America (Gibbs 1974; Benetti and Negreiros-Frasozo 2004; Benetti et al. 2007). Hampton et al. (2014) found a significant difference in the carapace structure of female *M. burgersi* populations from northern and southern Brazil. The northern crabs exhibited swelling in the hepatic region when compared to the southern populations. To give a broader geographic perspective, the present study examines the relationship between the geographic distribution and both phenotypic and genetic variation among *M. burgersi* populations across its range in the western Atlantic Ocean. Allometric data from 1153 individuals were analyzed quantitatively across the two geographic regions (Table S1a). Carapace shape was analyzed in 39 populations (Table S1b) using geometric morphometrics and correlated with three habitat variables: salinity, substrate, and location. Finally, an analysis of DNA sequences for mitochondrial 16S rDNA and cytochrome oxidase 1 (*COI*) was used to examine the genetic diversity in 25 populations in the western Atlantic Ocean (Table 1). Altogether, this data is used for a more complete assessment of the variation in *M. burgersi* across its biogeographic distribution.

MATERIALS AND METHODS

Specimens

Specimens used for this study were collected by CLT between 1976 and 2018. In total, 1437 specimens of *M. burgersi* were collected and preserved from 105 locations along the shores of the western Atlantic Ocean between Florida and Southern Brazil (Fig. 1; Table S1). Of these locations, 42 were in the southeast United States, Mexico, Belize, Jamaica, Puerto Rico, US Virgin Islands (St John and St Thomas), San Salvador Island in the Bahamas, St Martin, Belize, Guatemala, Barbados, Aruba, Curaçao, Trinidad and Tobago. More than 600 specimens were preserved (563 males, 100 females) from the sites in North America and the Caribbean.

In 2009 and 2010, 63 locations were visited along the Atlantic coast of Brazil. More than 800 specimens (583 males, 221 females) were preserved from Brazil. In most cases, the specimens were used initially in physiological studies (Thurman 2002 2003a b; Thurman et al. 2010 2017). Afterwards, they were euthanized by freezing, preserved in 80% ethanol, and deposited into the collection of the Department of Biology, University of Northern Iowa (UNI) or the Zoological Museum, University of São Paulo (ZMUSP).

Specimens from all regions were used for morphometric analysis (Table S1). Voucher specimens of *M. burgersi* from (1) the National Museum of Natural History, Washington, DC, USA (USNM); (2) the Zoological Museum, University of São Paulo, São Paulo, Brazil (ZMUSP); and (3) Rijks Museum, Leiden, the Netherlands (RMNH) were examined to authenticate the species characteristics. Additional specimens from the Zoological Collections of the Department of Life Science, National Chung Hsing University, Taichung, Taiwan (NCHUZOOL) and the Zoological Reference Collection of the Lee Kong Chian Natural History Museum, National University of Singapore (ZRC) were included in the molecular study. The locations and sources of preserved museum specimens are listed in the supplementary material (Table S1).

Allometric analysis

A total of 922 males, 226 females and 7 juveniles from 44 populations distributed throughout the Caribbean and Brazil were used to analyze anatomical relationships (Table S1a). These were sorted into a Caribbean island group ($n = 622$) and a South American group ($n = 531$). Digital calipers were used (by CLT and REA) to measure, to the nearest 0.01 mm, carapace width (CW), carapace length (CL), large claw length (LCL), propodus length (PrL) and pollex length (PoL) in each male exhibiting normal morphology (Figs. 2, 3). If the claw appeared to be regenerated (*i.e.*, abnormally small) or broken (Jones 1980), the specimen was excluded from the study. Carapace width (CW), carapace length (CL), abdominal width (AW) and small claw length (SCL) were measured for females exhibiting normal morphology. In general, all measurements were sorted into size intervals based on CW.

Geometric morphometric analysis

Morphological variation in carapace shape was assessed using geometric morphometric methods (Bookstein 1991; Zelditch et al. 2012). Since males have an asymmetrical carapace due to the growth of the enlarged cheliped, females were used to minimize the

Table 1. Haplotypes of 16S rDNA and *COI* markers for specimens of *Minuca burgersi* from the Americas, and the related outgroups

| Species | Locality | Catalogue no. of UNI (unless indicated) | Sample size | Haplotype of 16S | Access. no. | Haplotype Access. no. of <i>COI</i> |
|--------------------|---|--|----------------|---------------------|-------------|---|
| <i>M. burgersi</i> | | | | | | |
| Clade 1 | Trinidad: Maracas Bay Village | 3463 | 1 | bu11 | LC150347 | bu-C11a MW311038 |
| | Trinidad: Maracas Bay Village | A3464 | 1 | bu12 | MW310187 | bu-C12 MW311039 |
| | Trinidad: Blanchissuese | 3457 | 1 | bu11 | LC150347 | bu-C11b MW311040 |
| | Trinidad: Invader's Bay | 3491 | 1 | bu13 | MW310188 | bu-C13 MW311041 |
| | Brazil: Maranhão: Icatu | 2818 | 1 | bu11 | LC150347 | bu-C11c MW311042 |
| | Brazil: Ceará: Fortaleza | 2401 | 1 | bu14 | MW310189 | bu-C14 MW311043 |
| | Brazil: Pernambuco: Porto de Galinhas | 143 | 1 | bu11 | LC150347 | bu-C11d MW311044 |
| | Brazil: Bahia: Madre de Deus | 965 | 1 | bu15 | MW310190 | bu-C15 MW311045 |
| | Brazil: Espírito Santo: Guarapari | 403 | 1 | bu11 | LC150347 | bu-C11e MW311046 |
| | Brazil: Rio de Janeiro | NCHUZOO1 13956 | 1 | bu11 | LC150347 | bu-C11f LC150407 |
| | Brazil: Rio de Janeiro | NCHUZOO1 13956 | 1 | bu16 | MW310191 | bu-C11c MW311042 |
| | Brazil: Rio de Janeiro | NCHUZOO1 13956 | 1 | bu11 | LC150347 | bu-C11g MW311047 |
| | Brazil: Rio de Janeiro | NCHUZOO1 13956 | 1 | bu11 | LC150347 | bu-C11h MW311048 |
| | Brazil: São Paulo: São Sebastião | 2603 | 1 | bu11 | LC150347 | bu-C11c MW311042 |
| | Brazil: Paraná: Guaratuba | 1643 | 1 | bu11 | LC150347 | bu-C11i MW311049 |
| | Brazil: Santa Catarina: Florianópolis | 1887 | 1 | bu11 | LC150347 | bu-C11j MW311050 |
| Clade 2 | USA: Florida | 486 | 1 | bu21 | MW310192 | bu-C21a MW311051 |
| | Belize: Stann Creek: Sittee Point | 73 | 1 | bu21 | MW310192 | bu-C21b MW311052 |
| | Belize: Stann Creek: Sittee Point | 116 | 1 | bu22 | MW310193 | bu-C22 MW311053 |
| | Bahamas: San Salvador: Pigeon Creek | 1880 | 1 | bu23 | MW310194 | bu-C23 LC087950 |
| | Bahamas: San Salvador: Salt Pan | ZRC | 3 | bu24 | LC087920 | bu-C23 LC087950 |
| | Jamaica: St. Ann Parish | 201 | 1 | bu25 | MW310195 | bu-C25 MW311054 |
| | Jamaica: St. Ann Parish | 201 | 1 | bu26 | MW310196 | bu-C26 MW311055 |
| | Dominican Republic: Sanchez | | 1 | — | | bu-C27 FN430703 |
| | U.S. Virgin Islands: Princess Bay | 1609 | 1 | bu28 | MW310197 | bu-C28 MW311056 |
| Clade 3 | Bahamas: San Salvador: United Estates | 1884 | 1 | bu31 | MW310198 | bu-C31 MW311057 |
| | Bahamas: San Salvador: Pigeon Creek | 1881 | 1 | bu32 | MW310199 | bu-C32a MW311058 |
| | Bahamas: San Salvador: Pigeon Creek | 1879 | 1 | bu33 | MW310200 | bu-C33 MW311059 |
| | Puerto Rico: Río de la Plata | 2729 | 1 | bu34 | MW310201 | bu-C32b MW311060 |
| | Puerto Rico: Cabo Rojo | 2759 | 1 | bu32 | MW310199 | bu-C32b MW311060 |
| | U.S. Virgin Islands, St. Thomas, Fortuna Bay | 1590 | 1 | bu32 | MW310199 | bu-C32c MW311061 |
| | U.S. Virgin Islands: St. Thomas: Perseverance Bay | 1560 | 1 | bu35 | MW310202 | bu-C35 MW311062 |
| | U.S. Virgin Islands: St. John: East End | 1593 | 1 | bu32 | MW310199 | bu-C32b MW311060 |
| | Barbados: St. Lucy: Maycocks Bay | 3345 | 1 | bu32 | MW310199 | bu-C32d MW311063 |
| | Barbados: St. Peters: Reed's Bay | 3352 | 1 | bu32 | MW310199 | bu-C32e MW311064 |
| | Barbados: Christ Church | 3374 | 1 | bu36 | MW310203 | bu-C36 MW311065 |
| | Curaçao: Grote Knip (type locality) | 3316 | 1 | bu36 | MW310203 | bu-C32b MW311060 |
| | Curaçao: Charo | 3276 | 1 | bu37 | MW310204 | bu-C32b MW311060 |
| Total | | | 40 | | | |
| outgroups | | | | | | |
| <i>M. mordax</i> | Brazil: São Paulo | NCHUZOO1 13940 | mo1 | LC087923 | mo-C1 | LC087953 |
| | Brazil: São Paulo | NCHUZOO1 13940 | mo2 | MW310205 | mo-C2 | MW311066 |
| | Brazil: Santa Catarina: Itajai | B1838 | mo2 | MW310205 | mo-C1 | LC087953 |
| | Belize: Stann Creek: Sittee Point | 47 | mo3 | MW310206 | mo-C3 | MW311067 |
| <i>M. rapax</i> | USA: Florida | 2555 | ra1 | LC388593 | ra-C1 | LC087956 |
| | Brazil: Maranhão: Rio Crimã | B2855 | ra2 | LC388597 | ra-C2 | LC388620 |

influence of sexual selection (Hopkins and Thurman 2010). In all, 116 females were selected from 31 sites in the southeast United States, Mexico, Belize, Jamaica, Puerto Rico, US Virgin Islands (St. John and St. Thomas), San Salvador Island in the Bahamas, St. Martin, Belize, Guatemala, Barbados, Aruba, Curaçao, Trinidad and Tobago. In addition, 136 females were selected from eight locations in Brazil, for a total of 252 specimens sampled across the entire latitudinal range of the species complex (Table S1b). The female specimens were oriented for photography such that the carapace was horizontal in frontal view, and the anterior and posterior most edges of the carapace rested on the same horizontal plane in lateral view (Fig. 4A). All specimens were photographed by a single operator (MJH).

In total, 23 landmarks were chosen to represent the overall shape of the carapace and internal features of the crab (Fig. 4A, B). Landmarks were digitized (by REA) using ImageJ (Rasband 2018). Measurement error was evaluated to determine if inconsistent digitization was responsible for any significant variation

among specimens. This was done by photographing and digitizing a randomly chosen specimen twenty times, and then comparing this variation to the variation in the entire sample. The variation due to inconsistent digitization was at least one order of magnitude less than the intraspecific morphological variation, so digitization error was considered negligible and insignificant.

Shape data were prepared for analysis as described in Hopkins et al. (2016). Briefly, the symmetric component of variation was extracted following the method of Klingenberg et al. (2002) for object symmetry, and all the symmetric configurations were then superimposed jointly using generalized Procrustes superimposition. Specimens were grouped based on regions defined by distance and ocean current circulation (Caribbean, Mexico and Florida, northern Brazil, and southern Brazil), by locality substrate (carbonate, sandy mud, silty mud, and clay), and by local osmolality (hypersaline, eusaline, mesosaline, and oligosaline (Hedgpeth 1957)) based on $\text{mOsm kg}^{-1} \text{H}_2\text{O}$ readings from a Wescor Vapor Pressure osmometer

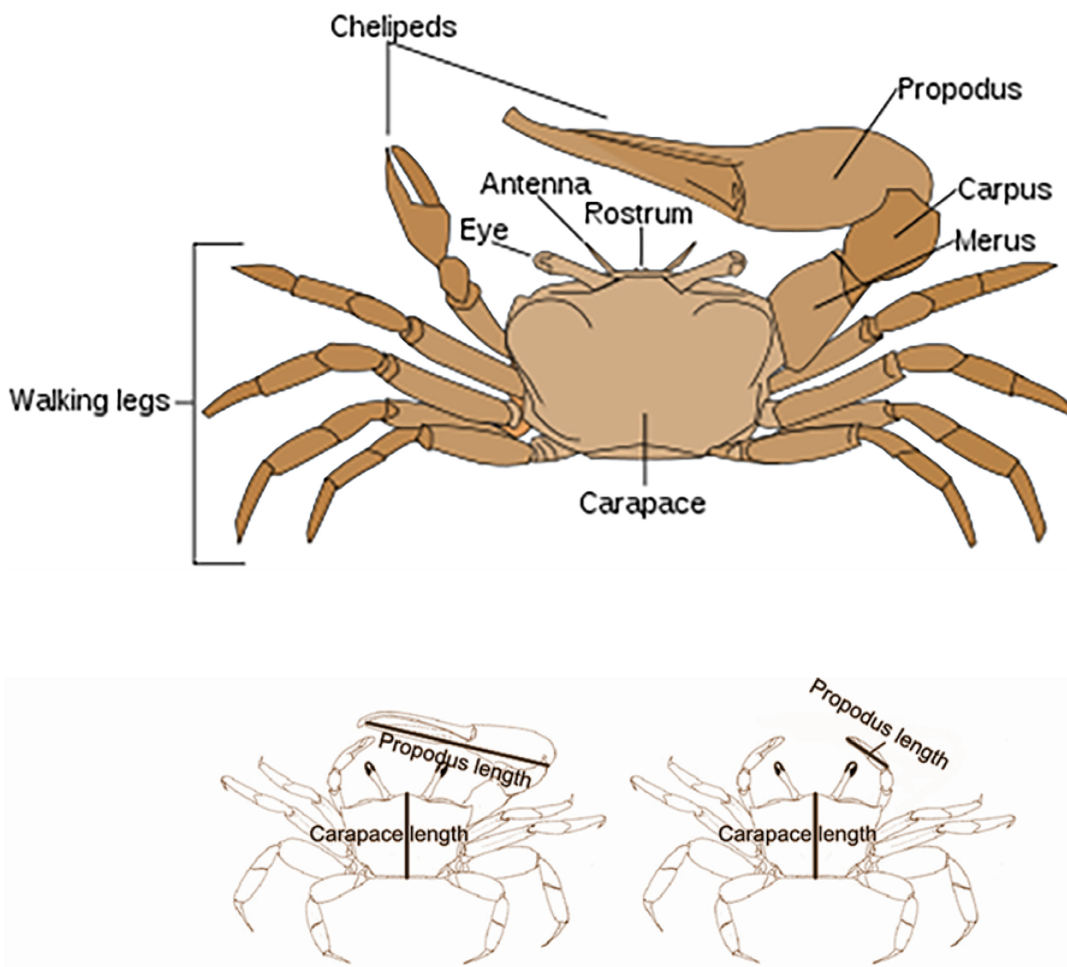


Fig. 2. Basic anatomy of *Minuca burgersi*.

(Thurman 2002) (Table S1b). Principal components analysis (PCA) of the Procrustes coordinates was used to summarize patterns of carapace shape among groups and thin-plate spline deformation plots were used to visualize the morphological variation summarized along each principal component. Initial data exploration was done using MorphoJ (Klingenberg 2011); subsequent analyses and figure generation were performed using the Geomorph 3.2.1 (Adams et al. 2020) and RRPP packages (Collyer and Adams 2018 2020) for the R statistical computing language (R Core Team 2020). Raw landmark data is available in dataset S1.

Analysis of DNA sequences

Forty *M. burgersi*, as well as the outgroups *M. mordax* and *M. rapax* (Shih et al. 2016), were used in the molecular study. Leg tissue samples were collected

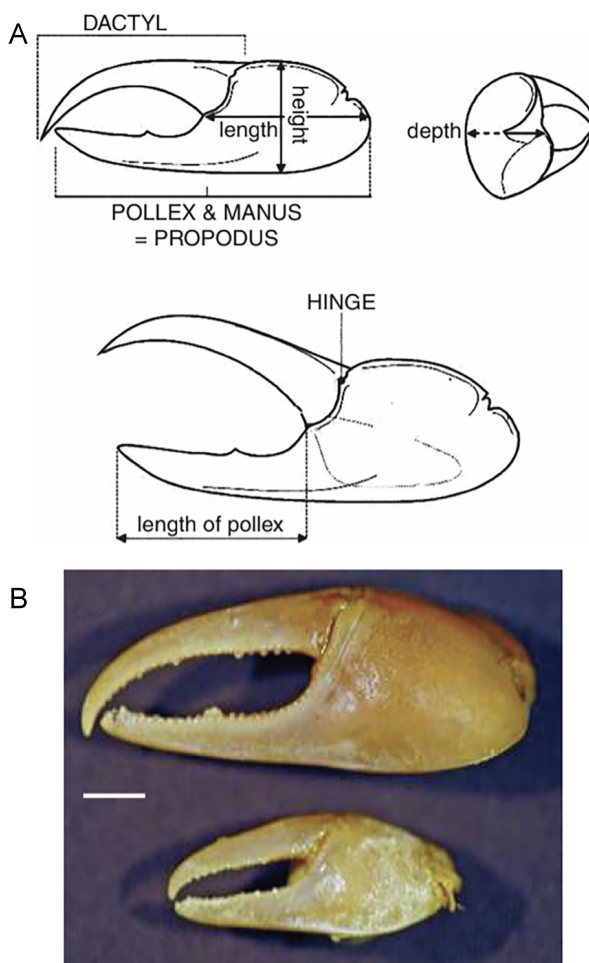


Fig. 3. Structure of major cheliped in *Minuca burgersi*. A, Relationship of pollex (PoL) and manus to total propodus length (PrL). B, General cheliped states: leptochelous (upper) and brachychelous (lower). Scale bar = 5.0 mm.

from 25 locations ranging from south Florida, Mexico, the Caribbean and Brazil (Table 1, Fig. 1). Specimens were preserved in 95% ethanol after collection and tissues were stored at -55°C until extraction. The sequences of mitochondrial 16S rDNA and cytochrome *c* oxidase subunit I (*COI*) were obtained following the method described by Shih et al. (2016), after verification with the complimentary strand. Sequences of the different haplotypes were deposited into the DNA Data Bank of Japan (DDBJ) (accession numbers in Table 1). An additional *COI* sequence from Dominican Republic (with GenBank accession number FN430703) was included in the haplotype network analysis (see below).

For the combined 16S and *COI* dataset, the best-fitting models for sequence evolution of individual datasets were determined by PartitionFinder (vers. 2.1.1, Lanfear et al. 2017), selected by the Bayesian information criterion (BIC). The best model, HKY+I, was subsequently applied for Bayesian inference (BI) analysis. The BI was performed with MrBayes (vers. 3.2.6, Ronquist et al. 2012). The search was run with four chains for 10 million generations and four independent runs, with trees sampled every 1000 generations. The convergence of chains was determined by the average standard deviation of split frequency values below the recommended 0.01 (Ronquist et al. 2019) and the first 1300 trees were discarded as the burn in. The maximum likelihood (ML) analysis was conducted in RAxML (vers. 7.2.6, Stamatakis 2006). The model GTR + G (*i.e.*, GTRGAMMA) was used for all subsets with 100 runs to find the best ML tree by comparing likelihood scores. The robustness of the ML tree was evaluated by 1,000 bootstrap pseudoreplicates using the model GTRGAMMA. The relationships of the *COI* haplotypes among populations of *M. burgersi* were examined using the program PopART (vers. 1.7, Leigh and Bryant 2015).

Statistical analysis

In all instances, the level of statistical significance was set at $p \leq 0.05$ for rejecting the null hypothesis. For allometric studies, corporal measurements were averaged and the standard deviation (SD) calculated for each size interval using Excel®. Best fit to a least-squares linear regression model illustrated relationships among most characters. SigmaPlot® was used for graphic plots of data. Regression to quadratic equations was determined with Sigma Plot. In geometric morphometric studies, the Mann-Whitney test and Procrustes MANOVA using a randomized residual permutation procedure (Collyer et al. 2015) and type III (marginal) sum of squares calculations (Shaw and Mitchell-Olds 1993) determined the significance

and interacting effect of size, region, substrate, and salinity on carapace shape. Because populations vary in maximum body size and some geographic variation may be due to differences in body size coupled with allometry (Hopkins and Thurman 2010), the natural log of centroid size was also included as a factor in the MANOVA. Alternatively removing the allometric

effect of size by regressing the superimposed symmetric configurations against the natural logarithm of centroid size and using the regression residuals in subsequent analyses (PCA and MANOVA excluding size as a factor) did not produce different results (Fig. S1 and Table S3).

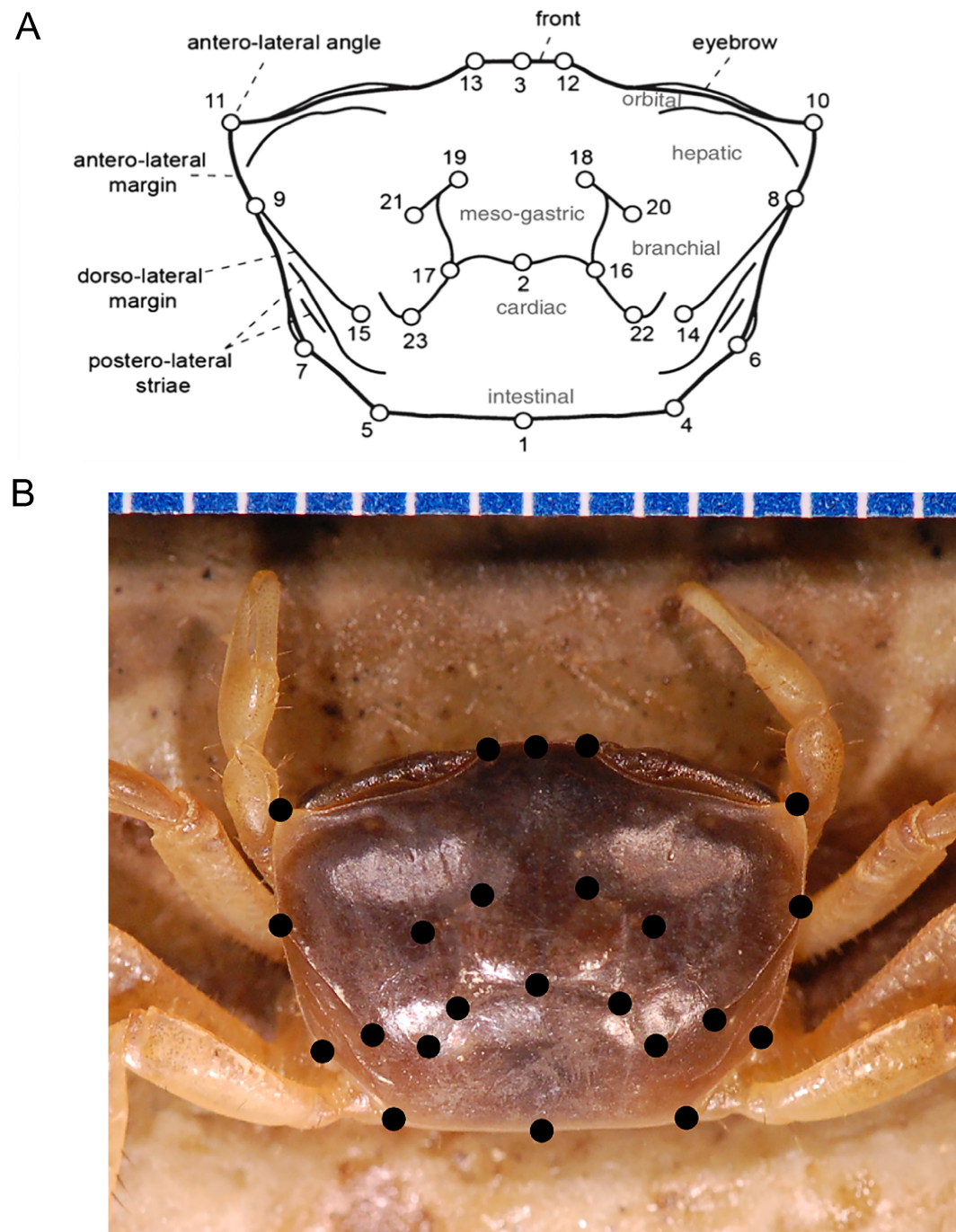


Fig. 4. Landmarks (total 23) chosen to summarize the shape of the carapace. A, Schematic of carapace showing anatomical features and landmarks. B, Photograph of *Minuca burgersi* specimen from Grote Knip, Curaçao. Scale above - white hatch marks are 1 mm apart.

RESULTS

Allometric analysis

Carapace width (CW): The CWs in Caribbean (N = 622) and South American (N = 531) populations of *M. burgersi* are shown in figures 5–7. Crabs from the

Caribbean (Fig. 5A) grow about 1 mm larger than those from Brazil (Fig. 5B). In the Caribbean, the CWs of *M. burgersi* usually vary between 6.00 mm and 20 mm in CW; mean \pm SD = 13.06 ± 2.63 mm. In South America the CW varies from 5.5 to 19 mm; mean \pm SD = 11.88 ± 2.89 mm. CW size-structure differs somewhat between Caribbean and South American *M. burgersi*. Across all

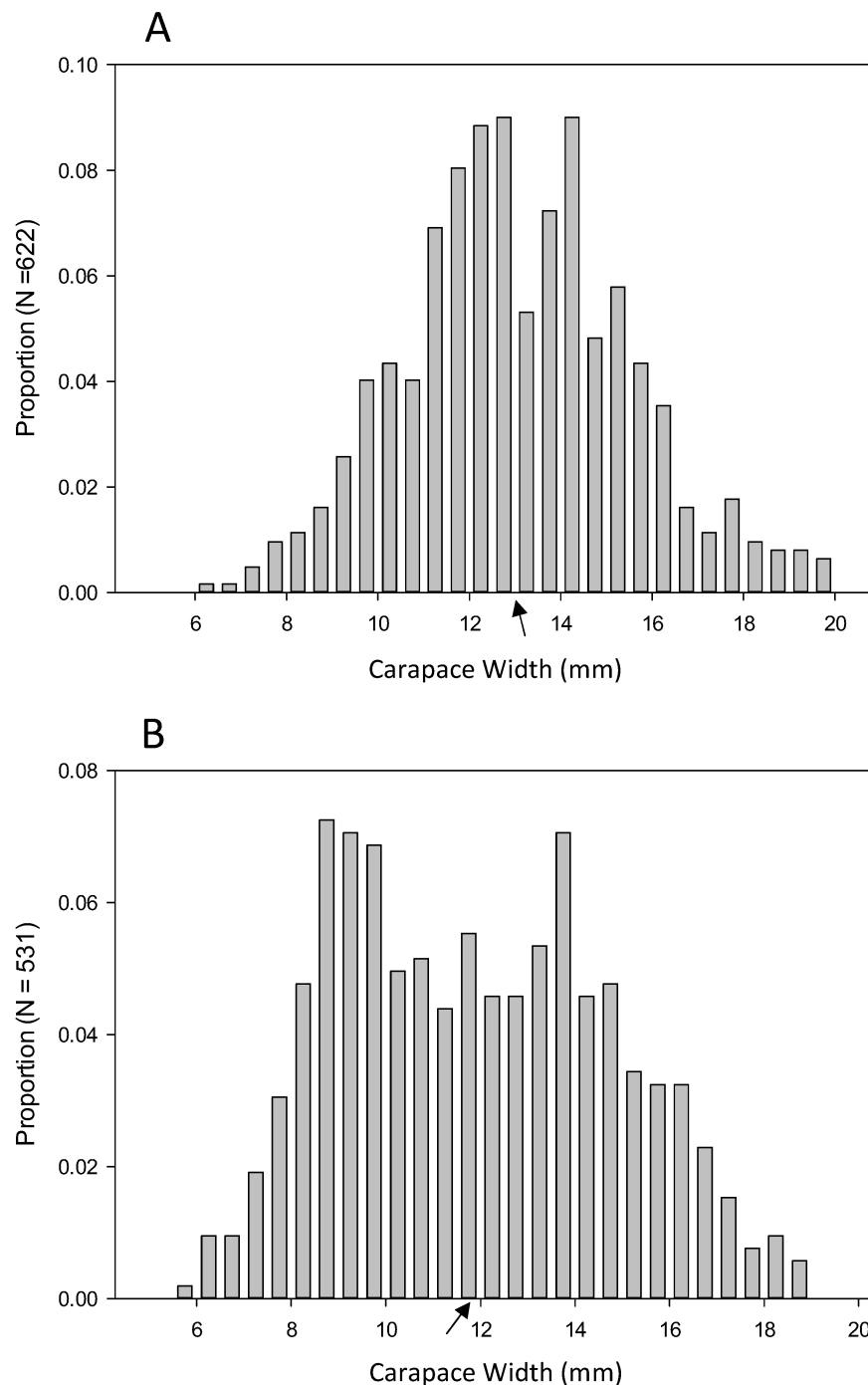


Fig. 5. Carapace widths for all *Minuca burgersi*. A, Caribbean populations. B, South American populations. Arrows indicate population mean CW.

populations, females range from 5.5 to 19 mm (Fig. 6), while males range from 6 mm to 19 mm (Fig. 7). The females from the Caribbean (Fig. 6A) are significantly larger (mean = 13.28 mm; N = 96) than females from South America (Fig. 6B) (mean = 11.37 mm; $p < 0.05$). Caribbean males are significantly larger than those from South America (Fig. 7B) ($d.f. = 925$, Student's $t = 4.78$,

$p < 0.001$). Using χ^2 to determine data dispersion, the CW measurements of Caribbean females are normally distributed ($\chi^2 = 33.46$, $d.f. = 31$, $p < 0.1$). Likewise, the distribution of CWs from Caribbean males (Fig. 7A) is unimodal ($\chi^2 = 31.87$, $d.f. = 30$, $p < 0.5$). On the other hand, South American females (Fig. 6B) and males (Fig. 7B) are not normally distributed (females: $\chi^2 =$

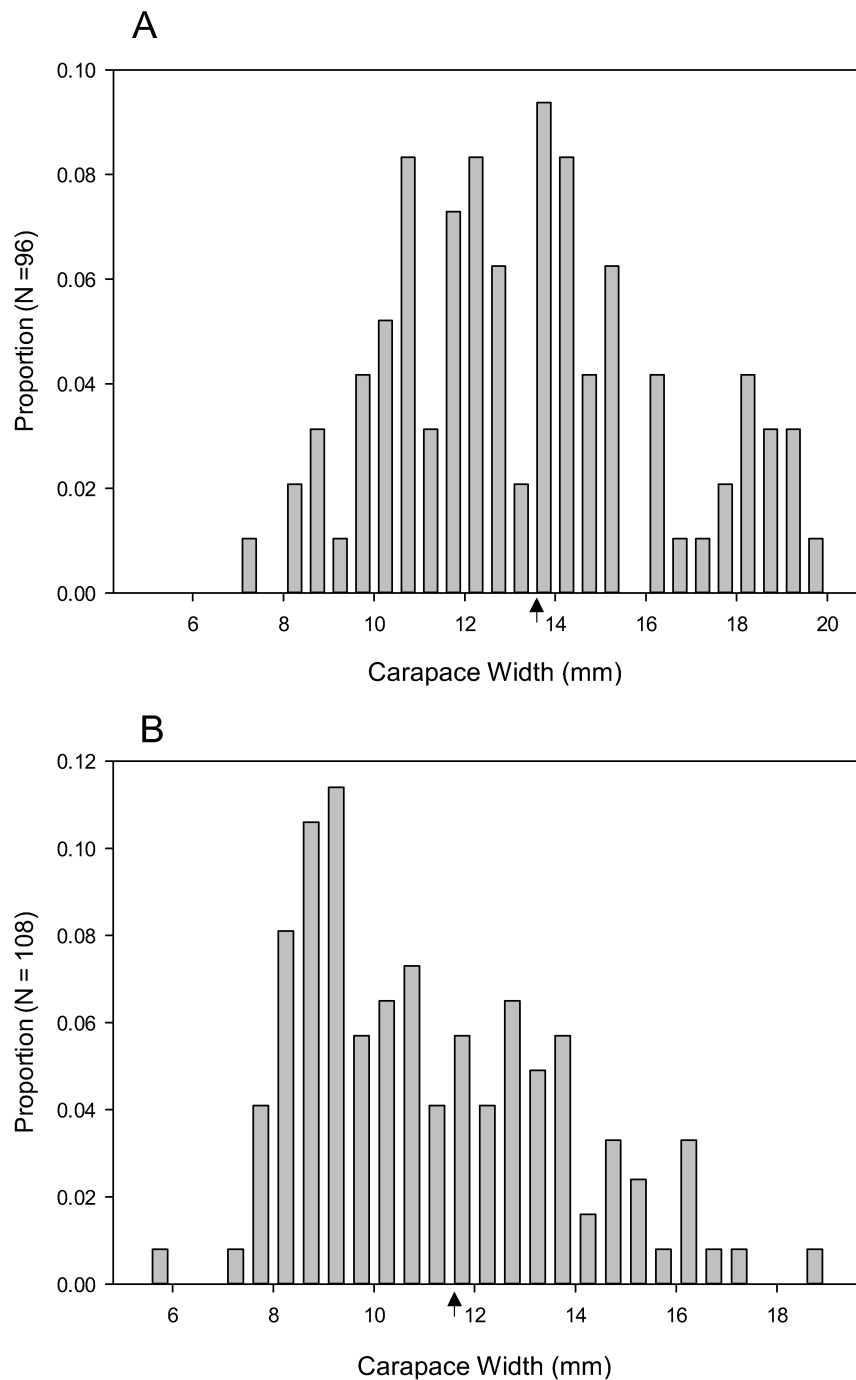


Fig. 6. Comparison of carapace width (CW) in female *Minuca burgersi*. A, Caribbean populations (N = 96); B, South American populations (N = 108). Arrows indicate mean values.

46.15, $d.f. = 27$, $p < 0.01$, males: $\chi^2 = 43.92$, $d.f. = 30$, $p < 0.05$). When examined with the Shapiro and Wilk test, both South American females and males deviated significantly from normality (females – $W = 0.96798$, $p = 0.0036$; males – $W = 0.97931$, $p = 0.000017$). Unfortunately, the number of CW measurements is insufficient for an accurate assessment of bimodal

distribution in the South American crabs. However, visual inspection of figure 6B implies that female CWs exhibit a “skewed” distribution with more individuals below than above the mean. The curve for South American males (Fig. 7B) appears platykurtic. There are fewer crabs than expected around the mean and more distributed toward the shoulders (Sokal and Rohlf

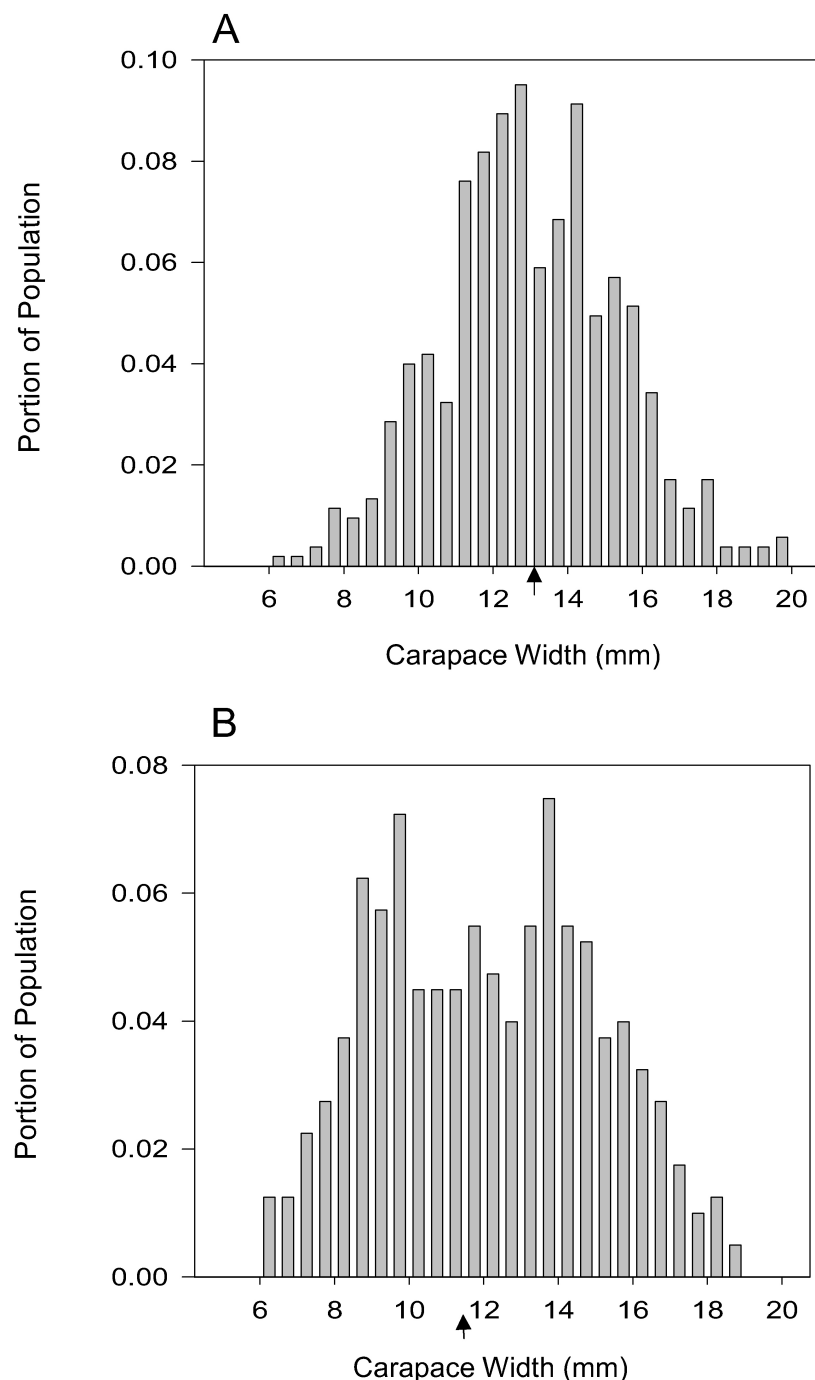


Fig. 7. Comparison of carapace width (CW) in male *Minuca burgersi*. A, Caribbean populations ($N = 526$), B, South American ($N = 401$). Arrows indicate average CW.

2012). In South American males (Fig. 7B), the 6 to 12.99 mm subpopulation had an average CW of 9.99 ± 1.70 mm while the 13 to 19 mm subpopulation had an average CW of 15.01 ± 1.41 mm.

Females

Carapace width (CW) and carapace length (CL): The linear relationship between CW and CL in female *M. burgersi* was explored in both Caribbean (N = 96) and South America (N = 108) populations. Figure 8 shows the average CL for each CW interval. The best-fit regression of CL with CW exhibits a highly significant correlation: Caribbean – d.f. = 11, $p < 0.001$, $r = 0.9930$, South America – d.f. = 10, $p < 0.001$, $r = 0.9930$. On average, CL is about 68% CW in females from both the Caribbean and South America.

Carapace width (CW) and small cheliped (claw) length (SCL): Figure 9 illustrates the linear relationship between average SCL for each 0.5 mm interval of CW in females. In both populations, SCL increases with CW in similar fashions (regression slopes 0.3436 and 0.3460). The correlations are significant (Caribbean – d.f. = 11, $p < 0.001$, $r = 0.9638$, South America – d.f. = 10, $p < 0.001$, $r = 0.9838$). However, for each carapace interval, average SCL is larger in South American than Caribbean female *M. burgersi*.

Carapace width (CW) and abdomen width (AW): Increase in AW is linear from 7 mm to 19 mm CW in females (Fig. 10). For Caribbean samples the linear regression is $AW = 0.9042 CW - 3.17$ mm (d.f. = 11, $p < 0.001$; $r = 0.9927$) while in the South American samples it is $AW = 0.8016 CW - 2.40$ mm (d.f. = 10,

$p < 0.001$; $r = 0.9970$). Essentially, the relationship is identical for Caribbean and South American populations. At 16 to 19 mm CW, the AW is slightly larger in Caribbean females. In smaller CW intervals (7 to 15 mm), there appears to be no difference in the CW to AW relationship between CW and CL the two *M. burgersi* populations.

Males

Carapace width (CW) and carapace length (CL): Figure 11 illustrates the linear relationship between CW and CL in males. Across both populations (Fig. 11), there is a significant correlation of CW with CL: Caribbean - CL = $0.6546 CW + 0.56$ mm (N = 521, d.f. = 12, $p < 0.001$, $r = 0.964$), South American - CL = $0.6956 CW + 0.52$ mm (N = 401, d.f. = 11, $p < 0.001$, $r = 0.9920$). On average, the CL of a male is approximately 66% of CW. CL per CW interval is slightly (but not significantly) greater in South American than Caribbean males.

Carapace width (CW) and large cheliped length (LCL): The linear relationship between CW and LCL is similar between the Caribbean and South American males (Fig. 12). On average, LCL enlargement occurs at twice the rate of CW expansion in both groups (Caribbean - LCL = $2.0932 CW - 9.47$ mm, d.f. = 11, $p < 0.001$, $r = 0.9188$; South America - LCL = $1.9623 CW - 8.14$ mm, d.f. = 10, $p < 0.001$, $r = 0.9970$).

Carapace width (CW) and large cheliped propodus to pollex length ratio (PPR): Figure 13 illustrates the non-linear relationship between CW and the PPR for males in both populations. Since the ratio compares

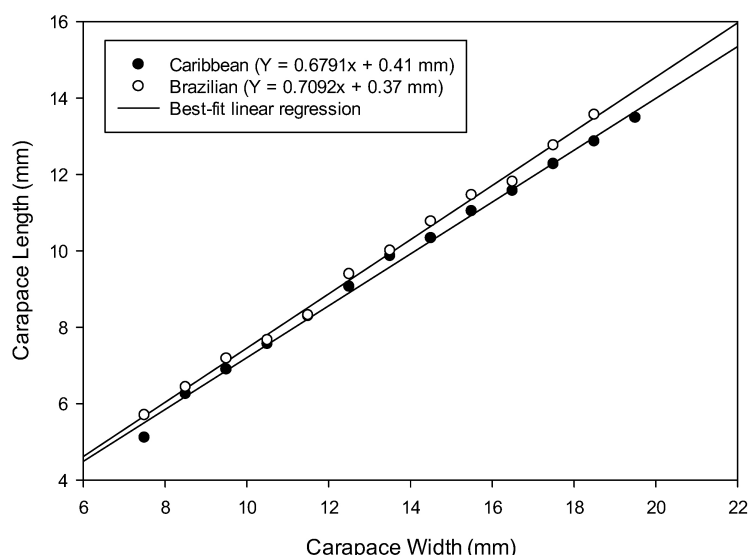


Fig. 8. Relationship between CW and CL in female *Minuca burgersi* in both Caribbean (N = 96) and South American (N = 108) populations. Data points calculated as average CL for each 1 mm interval of CW.

“claw” and “finger” lengths, there appears to be a critical CW size for the transition from a brachychelous to a leptochealous state (Fig. 3). In the Caribbean population the relationship is essentially linear from 6 to 15 mm ($PPR = 0.0056 \text{ CW mm} + 0.5440$ ($N = 520$, $d.f. = 7$, $p < 0.05$, $r = 0.7564$)). The quadratic regression is $y = 0.3506 + 0.0367x - 0.0011x^2$ ($r = 0.9866$). In the South American population, however, $PPR =$

$0.0175 \text{ CW mm} + 0.424$ ($N = 285$, $d.f. = 6$, $p < 0.001$; $r = 0.9983$) for male crabs 6 to 11 mm. For 12 mm to 19 mm CWs in the South American populations, the regression for males is $PPR = 0.0070 \text{ CW mm} + 0.8164$ ($N = 116$, $d.f. = 5$, $p < 0.05$, $r = 0.8165$). The quadratic regression is $y = 0.3506 + 0.0344x - 0.00097x^2$ ($r = 0.9793$). Based on comparing curve flexures, the rate of pollex elongation occurs at smaller CW sizes in South

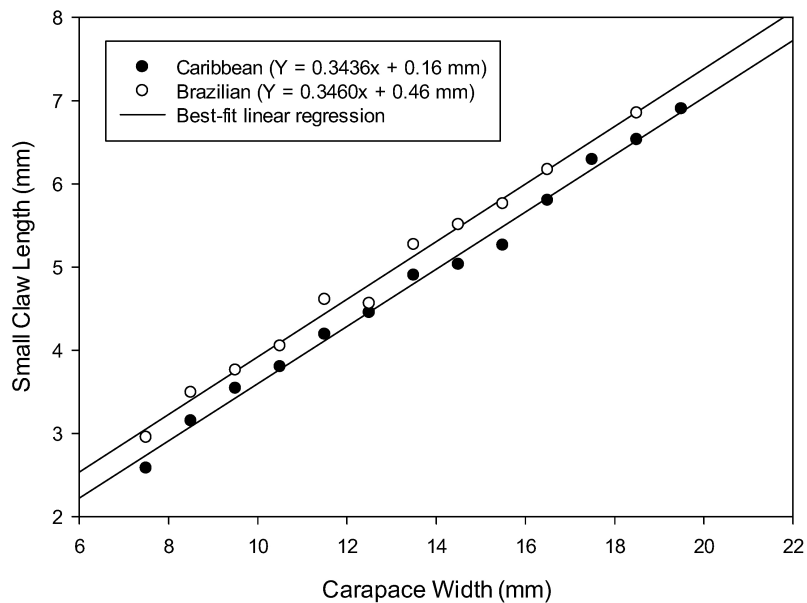


Fig. 9. Relationship between carapace width and small cheliped length in female *Minuca burgersi* from Caribbean and South American populations. Data points calculated as average SCL for each 1 mm interval of CW.

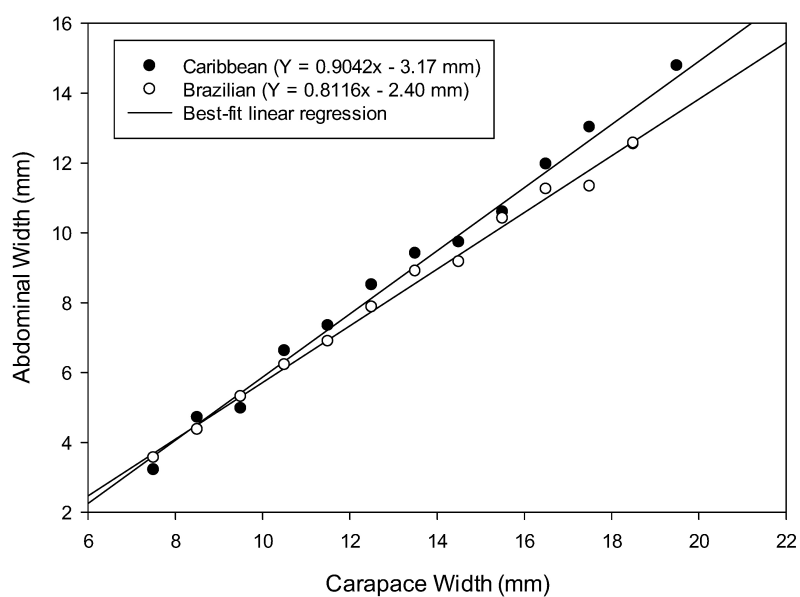


Fig. 10. Relationship between carapace width and abdomen width in female *Minuca burgersi* from Caribbean and South American populations. Data points calculated as average AW for each 1 mm interval of CW.

American (11 to 12 mm) than in Caribbean males (15 to 16 mm) (Fig. 13).

Large cheliped length (LCL) and the propodus to pollex length ratio (PPR): Figure 14 illustrates the non-linear relationship between average PPR and LCL. In both populations, a rapidly changing PPR is seen in male LCL intervals between 7 and 16 mm (PPR =

0.0081 LCL cm + 0.5178; *d.f.* = 10, *p* < 0.05, *r* = 0.6911). From CL intervals 17 to 34 mm, PPR = 0.0020 LCL mm + 0.6122 (*d.f.* = 15, *p* < 0.05, *r* = 0.0.3138). Comparing the slopes, the rate of elongation is over 4 times faster during early growth. For South American males, the cheliped is larger initially and grows rapidly to a 16–17 mm LCL transition interval (PPR = 0.00814 LCL

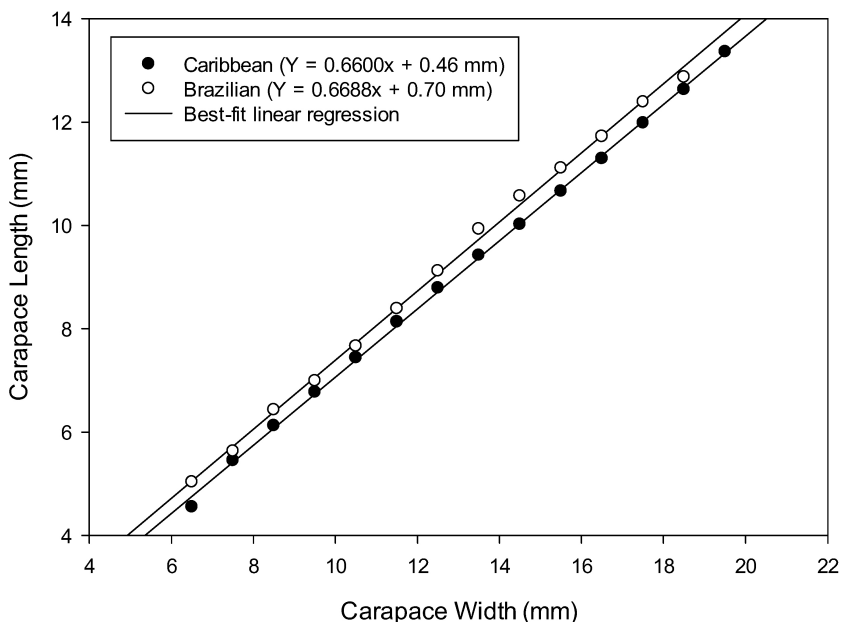


Fig. 11. Relationship between carapace width (CW) and length (CL) in male *Minuca burgersi* from both Caribbean ($N = 521$) and South American ($N = 401$) populations. Data points calculated as average CL for each 1 mm interval of CW.

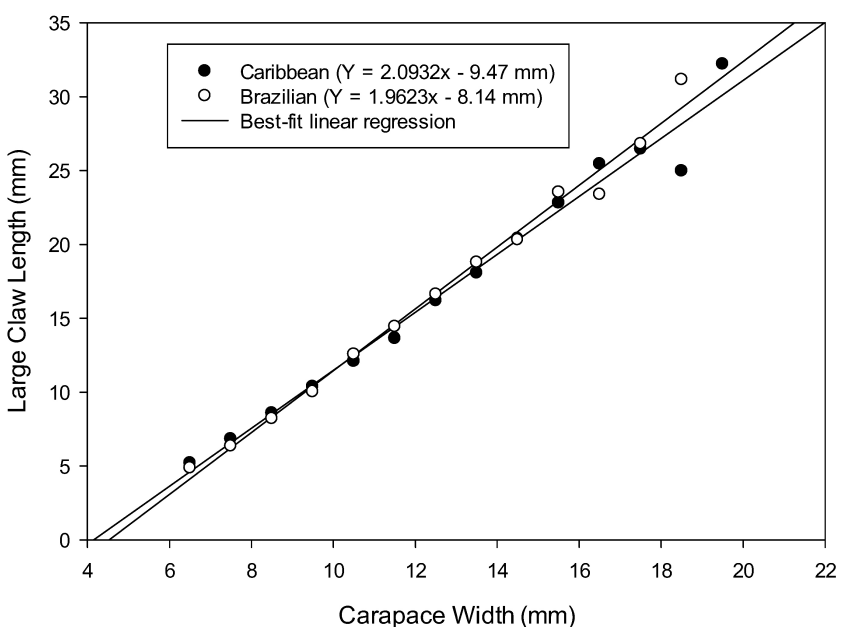


Fig. 12. Relationship between carapace width (CW) and large cheliped length (LCL) in male *Minuca burgersi* in both Caribbean and South American populations. Data points calculated as average LCL for each 1 mm interval of CW.

$+ 0.517$). The regression slope then declines in the 17 to 32 mm LCL interval ($PPR = 0.00195 LCL + 0.612$). In Caribbean males, a higher PPR slope occurs between CL of 4 to 21 mm ($PPR = 0.0085 LCL mm + 0.4885$, $d.f. = 15$, $p < 0.001$, $r = 0.9551$) then stabilizes from 22 to 35 mm ($PPR = 0.0067 LCL mm + 0.53421$; $d.f. = 12$, $p < 0.01$, $r = 0.83467$). Elongation occurs about 1.25

times faster in early compared to late growth. Quadratic regression for LCL to PPR in South American males is $y = 0.5516 + 0.0068x - 0.00010x^2$ ($r = 0.8900$) and Caribbean males it is $y = 0.4601 + 0.01431x - 0.00026x^2$ ($r = 0.9746$). Since average PPR is shifted to the left for South American males (Fig. 14), leptocheilous claws develop at smaller size-intervals for South American

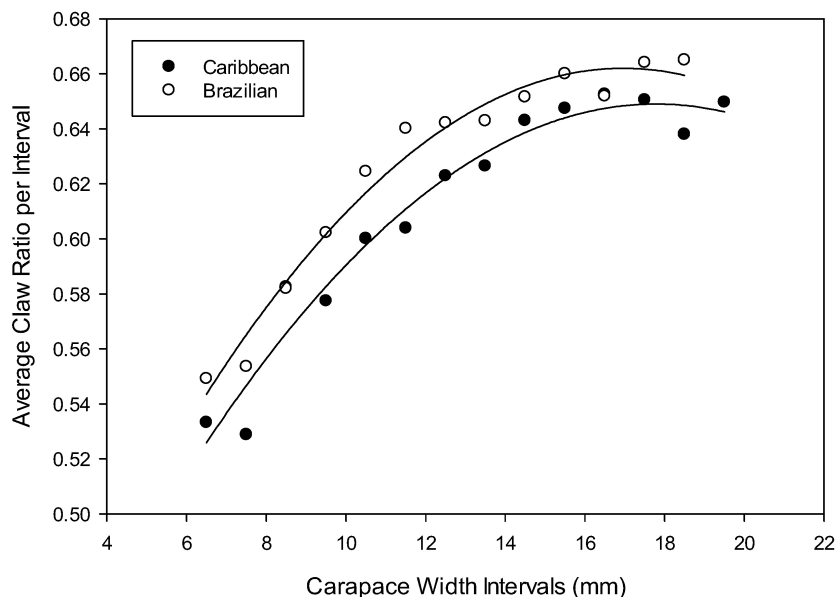


Fig. 13. Relationship between carapace width (CW) and propodus to pollex (PPR) ratio in male *Minuca burgersi* in both Caribbean and South American populations. Composite data calculated as average PPR ratio for each 1 mm interval of CW. Quadratic regression: South America $y = 0.3506 + 0.0344 x - 0.00097x^2$, $r = 0.9793$; Caribbean $y = 0.3506 + 0.0367 x - 0.0011 x^2$, $r = 0.9866$.

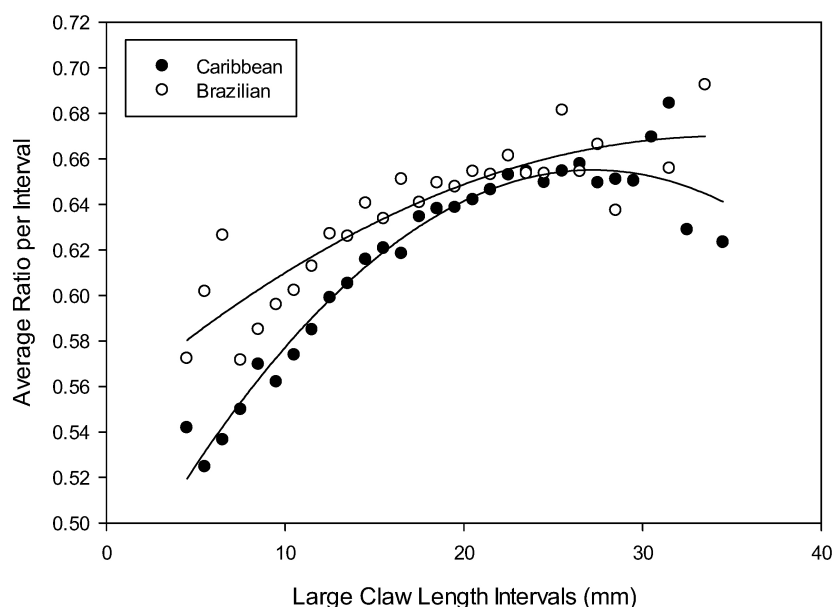


Fig. 14. Relationship between LCL and PPR ratio in male *Minuca burgersi* in both Caribbean and South American populations. Composite data calculated as average PPR ratio for each 1 mm interval of LCL. Quadratic regression: South America $y = 0.5516 + 0.0068 x - 0.00010 x^2$, $r = 0.8900$; Caribbean $y = 0.4604 + 0.01431 x - 0.00026 x^2$, $r = 0.9746$.

than Caribbean males *M. burgersi*. It is clear that this is an incipient property of cheliped growth (LCL) and, thus, related only secondarily to CW.

Geometric analysis

Size distributions among different geographic regions are broadly similar, with the exception of Florida/Mexico specimens, which are significantly larger (Fig. 15A; *p*-values from Mann-Whitney test $<< 0.001$, Table S2). Specimens sampled from carbonate substrates are larger than those sampled from terrigenous substrates (Fig. 15B; *p*-values from Mann-Whitney test < 0.05 , Table S2). The specimens collected from hypersaline environments are larger than the median size from meso- and oligohaline environments (Fig. 15C) but are still within the range sampled from both. The very low number of specimens sampled from hyper- and eusaline environments ($N = 3$ and $N = 1$, respectively) precludes any significance testing; there is no significant difference in size between specimens from oligo- and mesohaline environments (Mann-Whitney = 6734; *p* = 0.091).

The first two PCs summarize almost 50% of the total carapace shape variation in the dataset (Fig. S2). Specimens are most strongly clustered according to region (Fig. 15D), with South American specimens having higher PC1 scores and Mexican, Floridian, and Caribbean specimens having lower PC1 scores. The shape variation summarized along this axis is dominated by differences in the relative size of the branchial region at the expense of the size of the postero-lateral margin (Fig. 16). Caribbean specimens tend to have lower PC2 values compared with specimens from Mexico or Florida (Fig. 15D); there is also some separation among northern and southern South America specimens along this component with only specimens from southern Brazil occupying the space described by the highest PC2 scores. The variation described by PC2 is also dominated by differences in the relative size of the branchial region but at the expense of the hepatic region and the size of the antero-lateral margin (Fig. 16). The disparity (measured as sum of ranges across all PCs) is greater for Caribbean and southern Brazil groups than for Mexican/Floridian or northern Brazil groups (Table 2). Specimens are more moderately clustered based on substrate type with the greatest separation in carapace shape among specimens from carbonate vs. clay environments (Fig. 15E). There is almost complete overlap among groups based on salinity, although the three specimens sampled from hypersaline environments cluster together with lower PC1 values (Fig. 15F).

Because all specimens from carbonate environ-

ments are also from the Caribbean, Mexico, or Florida (compare Fig. 16D with Fig. 16E), an interaction term among the three factors was also included in the MANOVA. Results show that size, region, substrate, and salinity are all significant factors affecting carapace shape, but region has a much larger effect size (*Z*) than the other environmental factors (Table 3). The significant effect size of salinity is due to the inclusion of specimens from hypersaline and eusaline localities (note these specimens have lower PC scores in Fig. 15E). The small sample size in both groups, however, is unduly affecting the results, and if the MANOVA is rerun excluding these specimens, the *R*² value and effect size (*Z*) of salinity decreases and the *p*-value increases, without significant alteration to values for other factors (Table S3). As expected, there is a significant interaction between region and substrate type (Table 3).

Molecular genetics sequence analysis

A total of 20 haplotypes of 16S and 31 haplotypes of *COI* were identified in 40 *M. burgersi* specimens from both the Caribbean and Brazil (Table 1). Based on the phylogenetic tree of the combined 16S and *COI* (Fig. 17), *M. mordax* is sister to the “*M. burgersi* complex”. The complex is composed of three highly-supported clades, viz. Clade 1, Clade 2, and Clade 3. Although Clade 1 and Clade 2 are supported, the relationships among the clades are not clear. Clade 1 contains specimens from eastern South America (Trinidad to Santa Catarina, southern Brazil). Both Clade 2 and Clade 3 are dispersed around the Caribbean (Fig. 18a). Specimens from the type locality for *M. burgersi* on Curaçao are in Clade 3. For the *COI* haplotype network analysis, the shorter sequence from Jamaica (“bu-C26”) was excluded, but the Dominican Republic sequence (FN430703) was included. The network (Fig. 18a) shows that the three clades are separated by at least 25 steps, which is consistent with the clades revealed by 16S and *COI* (Fig. 17).

DISCUSSION

Morphological (phenotypic) differences may be related to the underlying allelic variation at one or more loci. Thus, allelic change can be reflected in phenotypic variation. Four forces manipulate genetic characteristics among and within populations: 1) disruptive/convergent selection, 2) mutation, 3) random drift, and 4) inbreeding (Wright 1930; Levins 1968). In the first instance, a critical environmental factor may select optimum phenotypes and genotypes to subsidize reproductive success in a particular habitat.

If successful, the second force produces new alleles and genotypes. For the third, allelic frequencies within a population may result from stochastic variation from one generation to the next. This can occur quickly when the breeding population is small and mating is

infrequent. Fourth, inbreeding results in reduced intra-population genetic diversity. For cases of inbreeding, within-population variance is small while among-population variance is much greater. For populations with extensive outbreeding, inter-population genetic

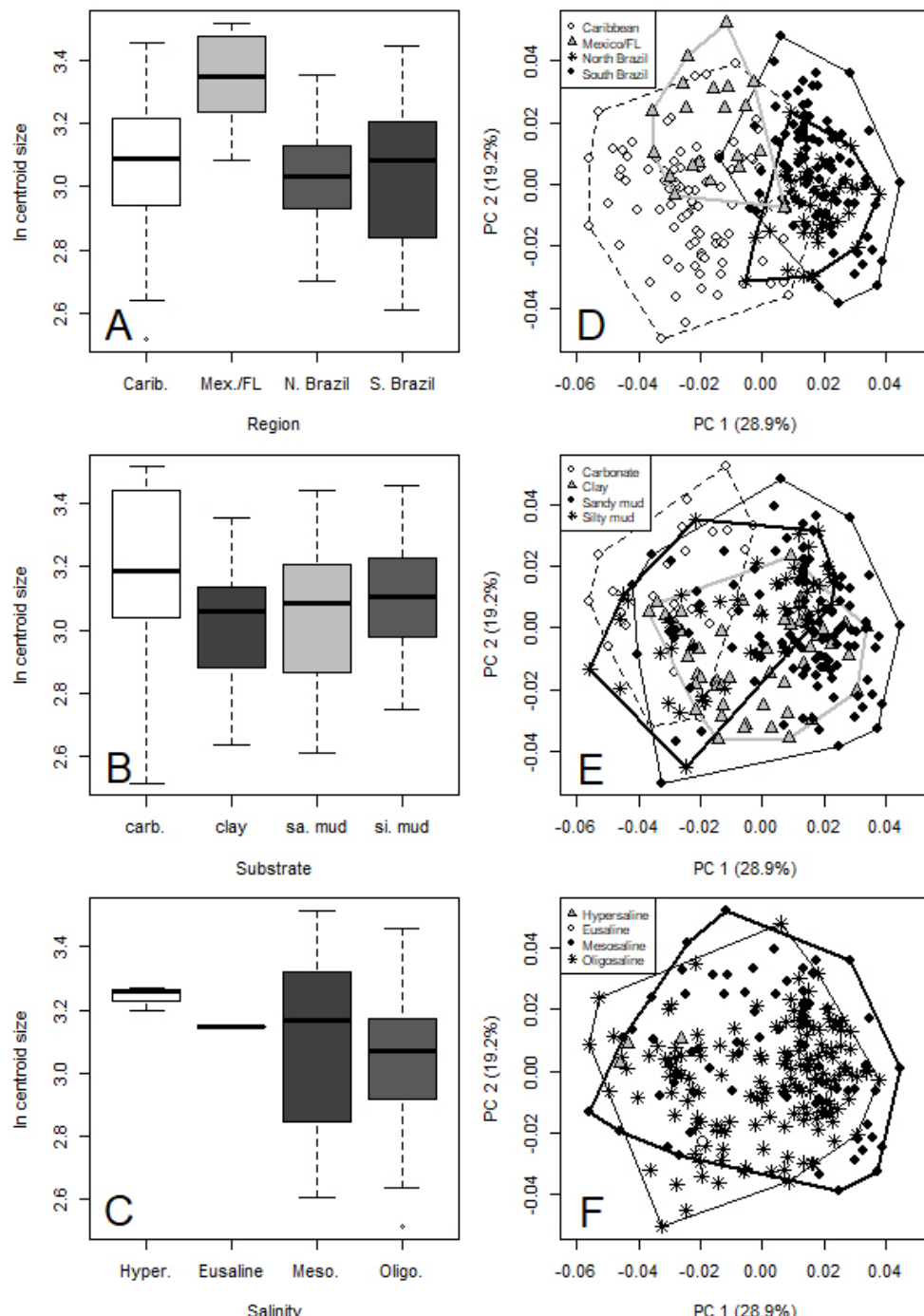


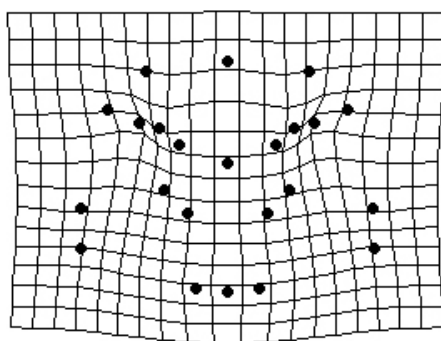
Fig. 15. Size distributions and principal components analysis of the landmark data. Size was measured as the natural log of the centroid size of the carapace. Boxplots (A-C) show median and interquartile range of size for each group, with whiskers extending 1.5 times the interquartile, and dots representing outliers beyond this range. Panels D-F show the first two principal components with different codings for each group. (A, D) Region. (B, E) Substrate. (C, F) Salinity.

variance is usually low and the intra-population variance is comparatively high (Wright 1930). Consequently, an examination of morphological and genetic traits across a species distribution could suggest which of these processes are acting to promote diversity in ecological adaption.

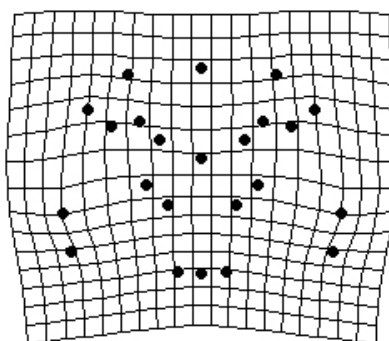
Over the last decade, several studies coupling global larval dispersal and gene flow in fiddler crabs have emerged: *Austruca annulipes* (Milne-Edwards 1837) (Silva et al. 2010), *A. triangularis* (A. Milne-Edwards 1873) and *A. perplexa* (H. Milne Edwards 1852) (Shih et al. 2019; Shih and Poupin 2020), *Paraleptuca crassipes* (White 1847) (Shih et al. 2012 2013), *Leptuca uruguayensis* (Nobili 1901) (Laurenzano et al. 2012) and *Uca maracoani* (Latrelle, 1803) (Wieman et al. 2014). Several species exhibit low genetic diversity across their ranges implying extensive connectivity via larval transport. On the other hand,

greater diversity and geographic structure has been documented in studies of *M. rapax* (Smith 1870) and *L. leptodactyla* (Rathbun 1898) (Laurenzano et al. 2013 2016; Thurman et al. 2018).

We have now assessed both morphologic and genetic diversity in populations of *M. burgersi*. After two morphological studies, Caribbean and South American populations were shown to exhibit a moderate level of divergence. In allometric assessments, Caribbean crabs are larger and their size-distribution is unimodal. On the other hand, South American crabs are smaller and have a bimodal size-distribution (Fig. 5). The cheliped of males in South America appears to elongate in smaller size-categories than in Caribbean crabs (Figs. 13, 14). We can speculate that South American males develop mature claws earlier enhancing their mating success and increasing opportunities for genetic investment (Greenspan 1980). From geometric



PC1



PC2

Fig. 16. Think-plate spline deformation plots showing the variation described by PC 1 (left) and PC 2 (right) shown in figure 15D–F.

Table 2. Extent of morphological diversity (disparity) within different sub-groups of specimens. Disparity is estimated as the sum of ranges of PC scores based on symmetric component of variation

| Group | Sum of Ranges |
|--------------|---------------|
| Caribbean | 0.752 |
| South Brazil | 0.731 |
| North Brazil | 0.599 |
| Mexico/FL | 0.554 |
| Silty mud | 0.704 |
| Sandy mud | 0.806 |
| Clay | 0.648 |
| Carbonate | 0.579 |
| Mesosaline | 0.760 |
| Oligosaline | 0.840 |
| Hypersaline | 0.223 |

Table 3. Results of MANOVA using a randomized residual permutation procedure (RRPP) and type III (marginal) sum of squares, which quantifies the effect of a particular factor adjusted for all other factors in the model (Shaw and Mitchell-Olds 1993). Effect sizes (Z) are standard deviations of observed SS-values from sampling distributions of random values found via RRPP. Residual degrees of variation = 221. See Table S3 for full additional statistics

| Factor | Df | Rsq | Z | P |
|--------------------|----|--------|---------|----------|
| size | 1 | 0.0866 | 34.6102 | > 0.0001 |
| region | 3 | 0.0949 | 12.6479 | > 0.0001 |
| substrate | 3 | 0.0375 | 4.9989 | > 0.0001 |
| salinity | 3 | 0.0185 | 2.4577 | 0.0005 |
| region:substrate | 4 | 0.0264 | 2.6337 | > 0.0001 |
| region:salinity | 1 | 0.0053 | 2.0994 | 0.0304 |
| substrate:salinity | 1 | 0.0034 | 1.3599 | 0.1926 |

analysis, overall carapace shape varies significantly between Mexico-Florida-Caribbean and Brazil specimens. Caribbean examples have less swollen branchial regions than those from South America (Fig. 16). Primarily, variation in carapace shape relates to geographic separation, with secondary influence from differences in substrate type. Molecular analysis revealed three clades (Figs. 17, 18). Data on Caribbean populations arose from crabs collected in Florida, Belize, Jamaica, Dominica, the Netherland's Antilles (Curaçao), Barbados, U.S. Virgin Islands, Puerto Rico, and the Bahamas (Fig. 17). The Caribbean haplotypes are unique and form two distinct genetic clades (Clade 2 and Clade 3), which may occur sympatrically on the same island (the Bahamas and U.S. Virgin Islands). The disparity in 16S and *COI* haplotypes between the two Caribbean clades implies that there are unknown "isolation" mechanisms operating among populations on the same island. Since 24 to 33 nucleotide steps separate the two clades from the South American clade (Fig. 18), the two clades are remotely related.

The most southern clade (Clade 1) includes disparate, unique haplotypes from Trinidad, Espírito Santo, São Paulo, Paraná, and Santa Catarina. These patterns of phenotypic and genotypic divergence imply that gene flow across the species range is restricted. It would be informative to know 1) where barriers are and 2) how long they have existed. In addition, 3) it would be interesting to speculate which environmental factors appear to exert selective pressures promoting diversity.

As to the first, we expected a major barrier to gene flow between the Caribbean and the Brazilian clades to be the freshwater and silt outflow from the both the Amazon and the Orinoco rivers into the Atlantic. This region is satisfactory for mud-loving fiddler crab species such as *U. maracoani*, *M. rapax*, *M. mordax*, *M. vocator*, *L. cumulanta*, and *L. thayeri* (Holthuis 1959; Thurman et al. 2013). However, species like *L. leptodactyla* and *M. burgersi*, which prefer sand, find no haven on these shores. In this study, we found the relationship among haplotypes from populations on Trinidad-Tobago and in Brazil to indicate that

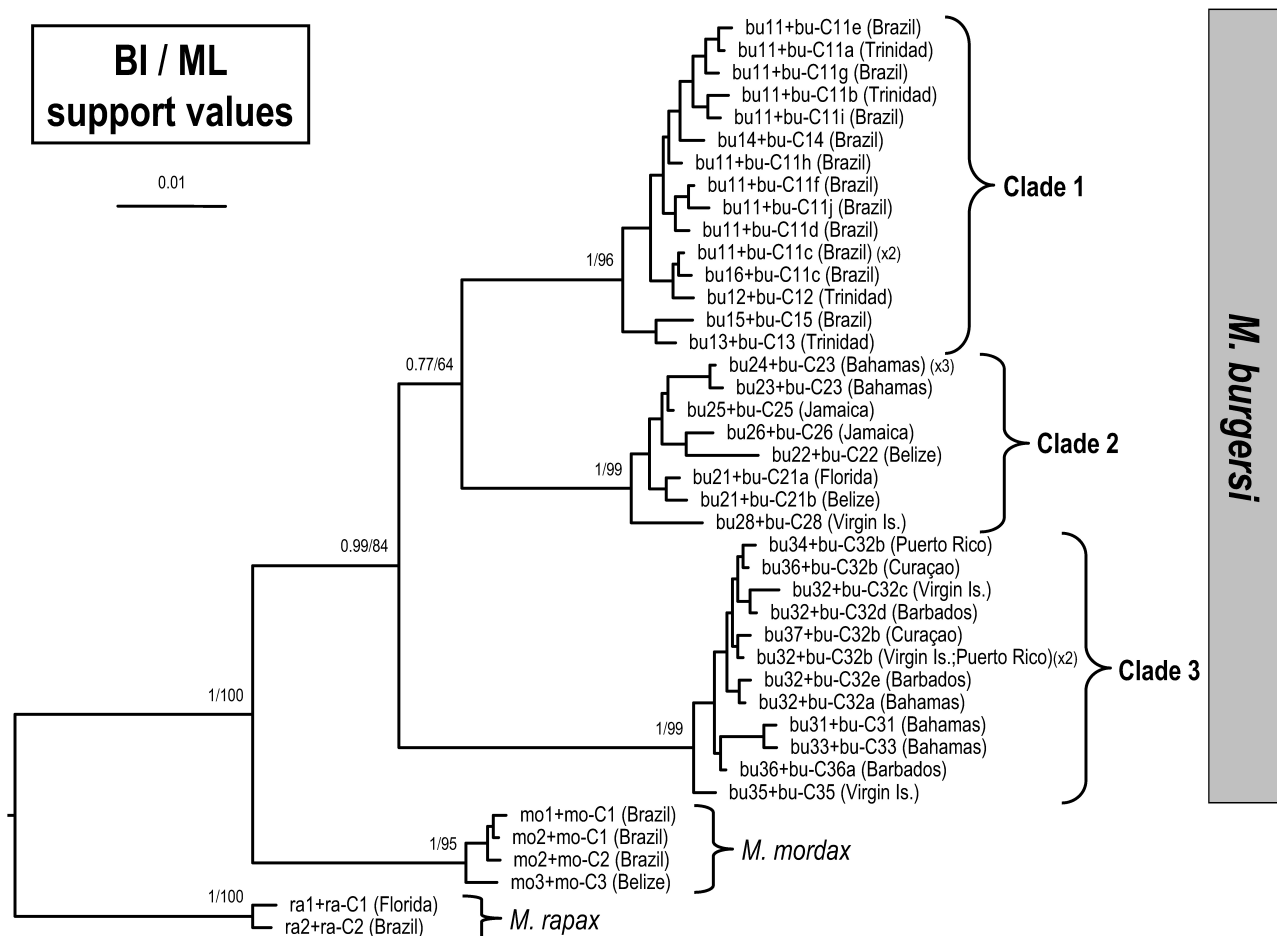


Fig. 17. A Bayesian inference (BI) tree for populations of *Minuca burgersi*, based on the combined 16S rDNA and cytochrome oxidase I. Probability values at the nodes represent support values for BI and maximum likelihood (ML). For haplotype names, see table 1.

the Amazon-Orinoco barrier is weak and locations are genetically connected. This may be due to larval development and its relevance to gene flow. Rieger (1998) and Vieira et al. (2010), describe larval and pre-adult development, respectively, in the juvenile stages of *M. burgersi*. On average, growth of zoea larvae occurs over 32 days. The duration of the two megalopae stages is approximately 8 and 13 days, respectively. The megalopae settle and become the first stage of the adult crab in 50 to 60 days. This very long planktonic phase would assure long-distance dispersal by the currents (Thurman et al. 2013). In light of the similarity between Trinidad and Brazil haplotypes, the planktonic larvae of *M. burgersi* appear capable of crossing the muddy shores formed by the Amazon River and Orinoco River

without settling. We calculate from hydrographic data (Borstad 1982) that planktonic transport from Pará or Maranhão, Brazil to Trinidad (~1509 km) by the Guyana Current (velocity ~36 km/day) would take 40 to 50 days. Apparently, there is sufficient time for larval transport from northeast Brazil to the Gulf of Paria where they can settle to become a remote enclave of reproductive adults on Trinidad. It is not clear why dispersion from this point north into the Caribbean is not continued. Larval flow through the Gulf of Paria via the Columbus Channel and the Bocas del Dragón into the Tobago Basin appears restricted.

The possibility that the Amazon and Orinoco serve as barriers to gene flow into the Caribbean was explored previously in *Leptuca leptodactyla* and *Minuca rapax*.

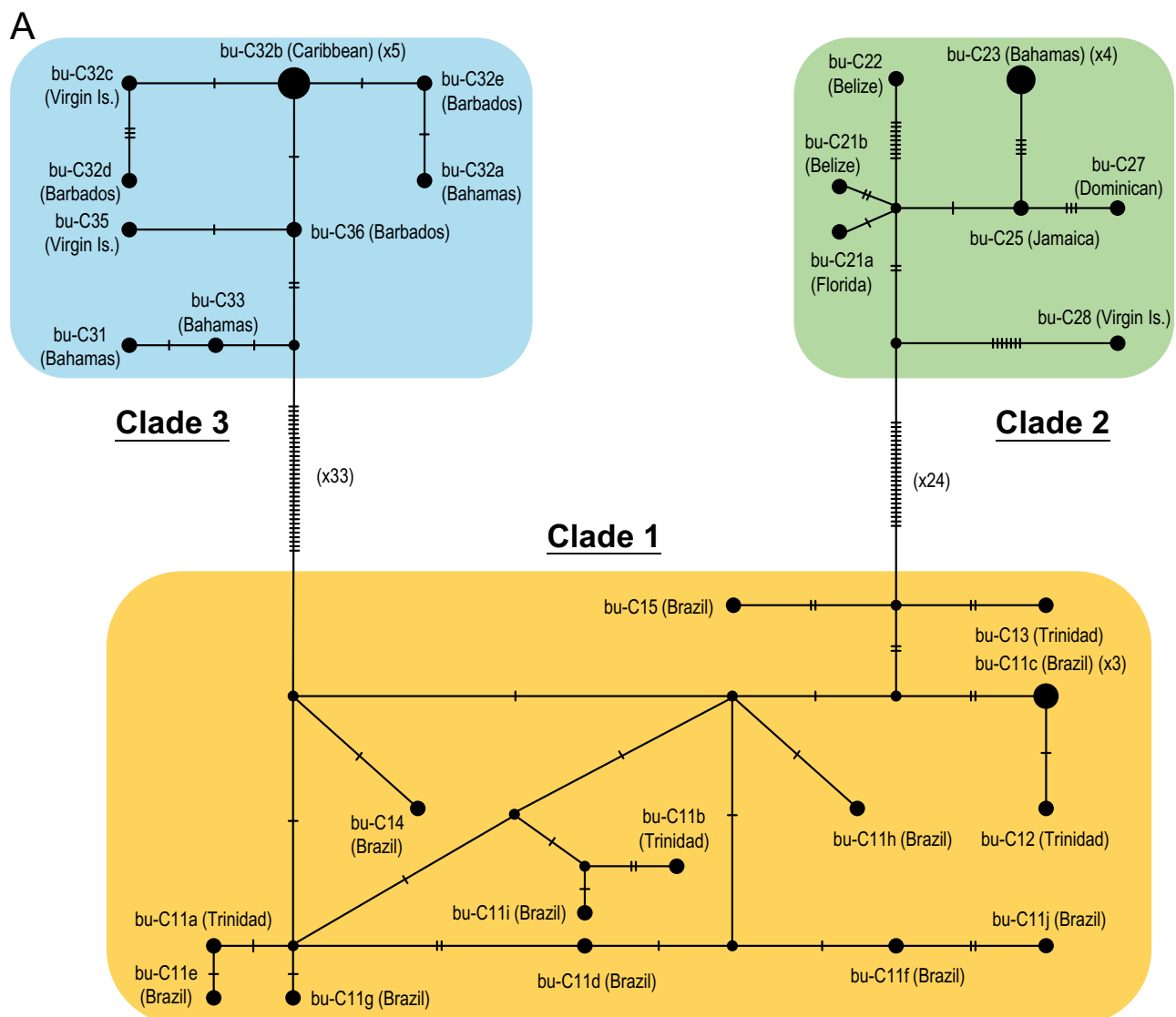


Fig. 18. A, Genealogical network for the *COI* haplotypes observed within the clades of *Minuca burgersi*. Unlabelled nodes indicate inferred haplotypes not found in the sampled population. Sizes of circles and squares are proportional to the frequency of the haplotype. For haplotype names, see table 1.

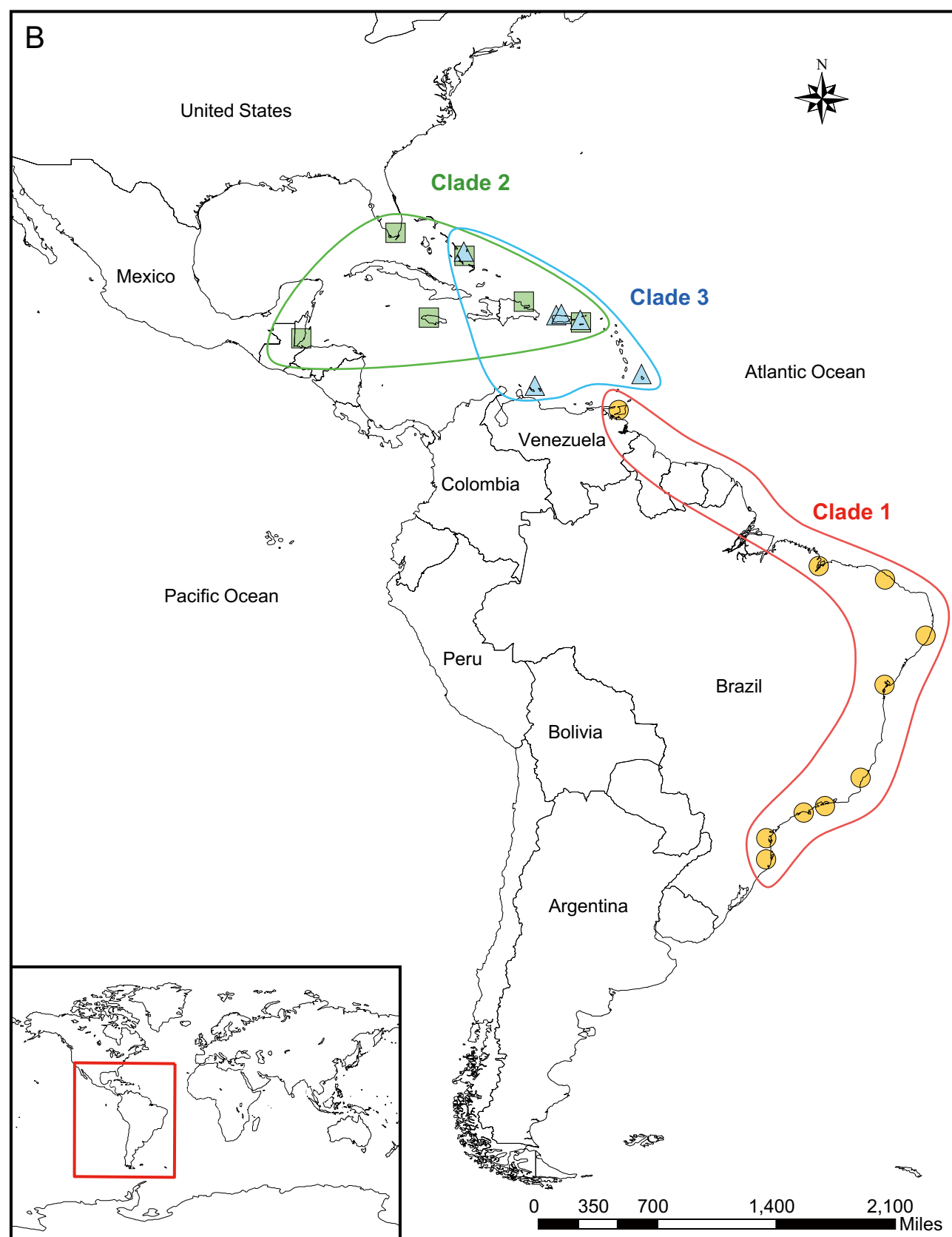


Fig. 18. B, The geographic distribution of three *COI* haplotypes clades.

Haplotype diversity is much greater along the coast of Brazil than between Caribbean Islands in the diminutive sand fiddler crab, *L. leptodactyla*. Since no *COI* haplotypes are shared between Caribbean and South American populations, the giant rivers of northeast South America appear to pose a significant barrier for the species (Laurenzano et al. 2016). Although we do not have precise development data, a close relative, *Leptuca uruguayensis* Nobili (1901), spends only 24 days as plankton (Thurman et al. 2013). If this is true for *L. leptodactyla*, it simply does not have sufficient dispersal potential to breach the Amazon-Orinoco barrier. *Minuca rapax* has been studied extensively (Holthuis 1957; von Hagen 1970b; Laurenzano et al. 2013 2016; Thurman et al. 2018) revealing a more complex structuring among populations. Those on the South American mainland are genetically indistinct (no barriers). However, four Caribbean populations (St. Martin, Hispaniola, Jamaica and Cuba) exhibit diverging haplotype frequencies indicating significantly restricted gene flow. There is also geographic divergence in carapace shape among north-central and southern Atlantic specimens of *M. rapax* (Hampton et al. 2014, Thurman et al. 2018). This variation manifested in the branchial region but was dominated by lateral compression of the region (see Thurman et al 2018: fig. 5C) rather than posterior expansion, as seen here for *M. burgersi* (Fig. 16). In the case of *M. rapax*, a weak barrier (filter) occurs between the South American mainland and the Caribbean while a more substantial barrier occurs among Caribbean islands (Lauranzano et al. 2013). In addition, substantial divergence (21 steps) is seen between populations in the western Gulf of Mexico separating *M. rapax* from “*M. virens*”. In the Gulf and Bahia de Campeche, the isolating mechanism may be persistent gyres in local currents (Thurman et al. 2018).

Second, as for geological age, to estimate the divergence time between South American and Caribbean *M. burgersi* populations, the nucleotide substitution rate of $1.17\% / 10^6$ year for the combined 16S and *COI* sequence data of marine crabs (cf. Schubart et al. 1998; Ragonieri et al. 2009; Shih et al. 2015) was applied to the *p*-distance between clades. The divergence time for *M. mordax* and *M. burgersi* (*p*-distance = $5.02\% \pm 0.56\%$) is 4.3 ± 0.5 million years ago (mya). Within *M. burgersi*, Clade 2 and Clade 3 diverged from each other 3.3 ± 0.4 mya (*p*-distance = $3.77\% \pm 0.5\%$). Clades 2 and 3 diverged from Clade 1 about 4.1 ± 0.5 mya (*p*-distance = $4.76\% \pm 0.57\%$). These temporal estimates are associated with geophysical events in central and eastern South America.

The freshwater outflow and sediment discharge from the Amazon River and adjacent rivers appear to

play an important role in restricting gene flow between the Caribbean and South American populations in many marine organisms (Floeter et al. 2008). The Amazon River developed in phases over the last 10 million years. There is evidence that the river has flowed into the Atlantic Ocean from the Andes for about the last 8.7 million years. However, major episodes of river capture as well as increasing uplift in the Andes due to ongoing tectonic activity, led to increased sedimentation rates around 4.5 mya (Latrubesse et al. 2010; van Soelen et al. 2017; Albert et al. 2018). Thus, restricted contact between the Caribbean clades (Clades 2 and 3) and the South American clade (Clade 1) occurred shortly after the Amazon started to drain water and sediments on a large scale into the Atlantic Ocean. The 4.3 mya divergence of *M. mordax* and *M. burgersi* could be linked to the periods of increased sedimentation along the coast. Segregation of Clade 1 from Clade 2 and Clade 3 is also intertwined with recent seismology and sedimentation in the region 4.1 mya during the Pliocene (Comeau 1991). Other marine species also show cladogenesis associated with the Amazon barrier around this same time (reef fishes, 6 mya, 4 mya and 1 mya; see Floeter et al. 2008; porcelain crabs, 2.5 mya; Hiller and Lessios 2017). Eventually, the flow of larvae into the eastern Pacific basin was eliminated around 3 mya by tectonic activity as the Isthmus of Panama and Gulf Stream formed (O’Dea et al. 2016; Jaramillo et al. 2017). This correlates with a 3.1 mya segregation between Clade 2 and Clade 3 during the late Pliocene. Their distributions may relate to weak larval exchange over the Mona Passage located between Puerto Rico and Hispaniola. The two clades overlap between the Bahamas and the Virgin Islands (Fig. 18B).

Third, are there clear ecological differences between *M. burgersi* in the Caribbean and South America? The habitat at the type location, Grote Knip, Curaçao, is a muddy mangrove lagoon in a coconut grove that is periodically inundated by tides (Holthuis 1967). On Dominica (Caribbean), it occupies areas with “no direct connection with the Caribbean and probably received salt water only during exceptionally high tides” (Chase and Hobbs 1969: 209). *Minuca burgersi* occupies several isolated lagoons on Barbuda that are two to three km from the coast (Gibbs and Bryan 1972; Gibbs 1974). On Trinidad, von Hagen (1970b) reported *M. burgersi* to be supra-tidal occupying sandy-mud near the mean high-tide mark. The two locations on Trinidad where we found *M. burgersi* are reminiscent of other Caribbean habitats with restricted connections to the sea. From a broader perspective, Crane (1975: 171) described the Caribbean biotope of the species as “characteristically well sheltered from open seawater, although always exposed to strong tidal influence...

never found upstream near the mangrove limits". By contrast, Coelho (1972) reported the habitat in Brazil as supra-littoral areas on low salinity rivers and estuaries. During our study in Brazil (Thurman et al. 2013), *M. burgersi* were collected upstream in rivers often sympatric with *M. mordax*. Consequently, we are led to suspect that the habitat preference of *M. burgersi* in the Caribbean and in South America are different. Below, we examine four habitat characteristic that could promote morphological and genetic divergence among *M. burgersi* in the Caribbean and South American: 1) aquatic basin, 2) tide amplitude/current, 3) salinity and 4) substrate.

Previous studies recorded size distributions in populations from isolated lagoons and along riverbanks. In a seminal study by Gibbs (1974), *M. burgersi* were found on Barbuda near the in the eastern Caribbean. Land-locked lagoons two to three kilometers from the sea possess the lowest salinity (Stoddard et al. 1978). Average CW is 10.43 mm but larger crabs are in low-salinity habitats. CW size-distribution varies from unimodal in males to bimodal in females. In Brazil, Benetti and Negreiros-Fransozo (2004) and Benetti et al. (2007) studied this species at two riverine locations along the coast of São Paulo. *Minuca burgersi* from riverbanks in Indaia and Cavalo were unimodal while those in Ubatumirim are bimodal. In spite of living in an isolated lagoon or on a riverbank, the size-distribution of adults is similar.

However, the two habitats appear to promote different strategies for larval development. If females release larvae into rivers and they are carried to the sea by the tide, genotypes can be widely broadcast by ocean currents. On the other hand, if the zoea have limited dispersal and develop in isolated lagoons by autochthonous descent (Gibbs 1974), genotypes will be localized and "patchy" in distribution. In the Caribbean, *M. burgersi* are found frequently in isolated, land-locked lagoons that are occasionally flooded by the highest tides. Genetic heterogeneity between the clades implies local "isolating" mechanisms. As a working hypothesis, the two Caribbean clades may result, in part, from different patterns of larval dispersal within the species. As in South America, some populations will use a long-distance dispersal strategy so the newly hatched zoea can be transported for long distances by currents. Populations on the continents and larger islands with rivers could employ planktonic dispersion. In other cases, parent crabs live around isolated, dry riverbeds or lagoons. Under these conditions, crabs would have limited dispersal potential and develop by autochthony. In support of this notion, Gibbs (1974) reports that the ova carried by Caribbean females were about 40% larger (340 to 380 μm) than those in other species (210

to 270 μm ; Crane 1941; Feest 1969). Given the isolated ecology of the crabs in mid-island, low-salinity lagoons, the enlarged ova implicate autochthonous descent (Gibbs 1974). This has proven to be the case in other semi-terrestrial crabs of the western Atlantic (Thurman 1979 1985; Rabalias and Cameron 1983; Schuh and Diesel 1995; Schubart et al. 1998). We speculate that the disparate genetic clades within Caribbean populations are the result of inbreeding, restricted gene flow and localized development. In some cases, the two habitat types (and dispersal strategies) may be adjacent to each other on the same island. Crabs just a few hundred meters apart would use different larval dispersal patterns and live in populations with different genetic structures. Unfortunately, ovum diameter data is lacking for *M. burgersi* from South America. In our Brazil study (Thurman et al. 2013), no females were collected with ova. None of the South American specimens from either the USNM or ZMUSP has ova to measure. Ovum diameter was not reported by Benetti and Negreiros-Fransozo (2004) or Benetti et al. (2007). Only seven females were ovigerous among 3810 crabs (0.18%). This indicates a low reproductive potential for *M. burgersi* in South America.

Another hydrographic variance between the Caribbean and South America is the tide amplitude and current. Tides are important in distributing larvae. The volume and velocity at any location is proportional to tidal height. Spring tide heights for locations in this study were estimated from tide charts (www.tide-forecast.com). The average tide amplitude for 11 locations in the Caribbean from south Florida to Barbados is 0.48 m (range 0.35 to 0.85 m), 0.73 m for Tobago, 1.15 m for Trinidad, and 3.039 m for eight locations on the east coast of South America (Guyana to Rio de Janeiro, range 2.04 to 5.45 m). Clearly, there is a stronger larval-motive force along the northeast coast of South America. The transition to a low amplitude tidal force occurs at the Tobago Basin and Barbados Trough in the southeast Caribbean. To the north, tidal currents are a weaker factor in planktonic dispersal. This would strengthen the concept of localized autochthonous development in Caribbean *M. burgersi* promoting genetic diversity.

Another pivotal factor regulating fiddler crab distribution is salinity or habitat osmolality (Thurman et al. 2017). It is believed that the Caribbean warmed and became more saline about 3 mya with uplifting of the Isthmus of Panama (O'Dea et al. 2016; Jaramillo et al. 2017). Thus, *M. burgersi* in the Caribbean would have needed to adapt to the elevated salinities. This may be one reason explaining the absence of *M. mordax* on Caribbean islands (von Hagen 1970a). Across the northern Caribbean, *M. burgersi* can be collected from

habitats with an average salinity of 454 ± 420 mOsm/kg H₂O ($15.1 \pm 14.0\%$) (Thurman et al. 2010). Many collection sites were land-locked lagoons. Thurman et al. (2013) found *M. burgersi* in Brazil in oligo- to mesohaline habitats with mean osmolality of 349 ± 79 mOsm/kg H₂O ($11.6 \pm 2.6\%$). It was commonly found cohabitating with *M. mordax* on the banks of streams or rivers. Unlike the Caribbean, none of the Brazilian sites had restricted or intermittent connections with the Atlantic Ocean. It was reported previously (Thurman et al. 2017) that *M. burgersi* in South America are frequently found in two different salinity habitats characterized by different means (\pm SD): 1) 144 ± 188 mOsm/kg H₂O ($4.8 \pm 6.2\%$) ($n = 3$) and 2) 394 ± 447 mOsm/kg H₂O ($13.1 \pm 14.9\%$) ($n = 5$). Another indication of acclimation to habitat osmolality is the hemolymph isosmotic concentration [ISO]. This is the concentration on the hemolymph-medium osmolality curve where the two are equal. In the Caribbean, the average (\pm SEM) [ISO] is 729 ± 44 mOsm/kg H₂O ($24.3 \pm 1.5\%$) (Thurman et al. 2010) while in South America the [ISO] is 691 ± 24 mOsm/kg H₂O ($23 \pm 0.8\%$). Although the [ISO]s are not significant ($p > 0.05$), there are different ecological and physiological challenges for crabs in the two regions. Interestingly, there are no significant differences in carapace shape relating to salinity (Fig. 15E, Table 3).

Finally, substrates are important to fiddler crabs in a variety of ways. Most species feed by placing

substrate particles in their buccal cavity and washing bacteria, algae and other nourishment from the grains (Miller 1961; Crane 1975). The types of setae on the second maxilliped and size of third maxilliped appear to be related to preferred substrates for feeding (Ono 1965; von Hagen 1970b). In the northern Caribbean (Thurman et al. 2010), *M. burgersi* is typically found inhabiting humus-rich silty mud sprinkled with chips of calcium carbonate. In south Florida and on the Yucatan Peninsula, it is collected from silty mud composed primarily of crushed coral. In Brazil (Thurman et al. 2013), it is collected from red-colored clay and sandy mud. However, in both locations, the habitat water is normally oligo- or mesosaline.

CONCLUSIONS

Using data from field collections and museum specimens, we examined intraspecific variation and diversity in *Minuca burgersi* across its range in the western Atlantic Ocean (Table 4). Allometric and geometric morphometric analyses were conducted on preserved specimens as molecular analysis of 16S and *COI* haplotypes was performed on isolated tissues. Each of the three approaches revealed significant regional phenotypic and genotypic diversity. Allometric analysis illustrate differences between Caribbean and South American populations. Through geometric analysis, four

Table 4. Summary of characteristics of *Minuca burgersi* Holthuis, 1967 from different regions. See text for discussion

| Character | Caribbean | Brazil |
|--|--|--|
| Typical habitat | land-locked lagoons | estuary and river banks |
| Substrate | limestone-rich, sandy soils | silty mud and clay |
| Typical salinity (mOsm kg ⁻¹ HOH) | 522 | 144–394 |
| [ISO] (mOsm kg ⁻¹ HOH) | 729 | 691 |
| Population CW structure | unimodal | bimodal |
| Avg. ♂ - CW (mm) | 13.06 ± 2.63 | 11.88 ± 2.89 |
| Avg. ♀ - CW (mm) | 13.28 ± 2.95 | 11.37 ± 2.55 |
| ♀ CL/CW % | 68 | 68 |
| Ova diameter (μm) | 340 to 380 | unknown |
| ♂ CL/CW % | 66 | 66 |
| Slope LCL vs CW ♂ | 2.107 | 2.093 |
| Pollex/propodus vs CW | non-linear | non-linear |
| Pollex/propodus vs LCL | slow development | rapid development |
| PPR transition interval LCL (mm) | 21–22 | 16–17 |
| Carapace shape | smaller branchial region | larger branchial region |
| Haplotypes of 16S (and <i>COI</i>) | <i>Clade 2</i> bu21, 22, 23, 24, 25, 26, 28 (bu-C21a, b, C22, C23, C25, C26, C27, C28) <i>Clade 3</i> bu31, 32, 33, 34, 35, 36*, 37* (bu-C31, C32a, b*, c, d, e, C33, C35, C36) | <i>Clade 1</i> bu11, 12, 13, 14, 15, 16 (bu-C11a, b, c, d, e, f, g, h, i, j, C12, C13, C14, C15) |

regional morphological clades emerged: 1) Mexico-Florida, 2) Caribbean islands, 3) northern Brazil and 4) southern Brazil. Based on molecular analysis, three regional genetic clades are evident: 1) South America, 2) southern Caribbean and 3) northern Caribbean. While differences in substrate, habitat osmolality and, perhaps, temperature are minor factors contributing to diversification in *M. burgersi*, the most prominent factors are ocean current patterns and tidal amplitude due to their presumed impact on larval distribution. A marked transition from a high to low larval-motive force occurs between Trinidad-Tobago and Grenada in the extreme southeast Caribbean. A second barrier to gene flow may reside at Mona Passage between Puerto Rico and Hispaniola. Along with subtle environmental factors, oceanographic barriers are instrumental in facilitating intraspecific diversity across the range of *M. burgersi*.

Acknowledgments: Portions of this research were included in a UNI Biology Honors thesis (by REA) supported by a 2018-19 award from the Dr. Gary and Myrna Floyd Undergraduate Research Assistantship Fund (UNI). Collecting expenses incurred (by CLT) in Barbados, Curaçao, Trinidad, and Guyana were deferred in part by a gift from Emily VanLaar to the UNI Department of Biology Undergraduate Research Fund. Cultural Insurance Service International (CISI) travel protection (for CLT) provided by the UNI Study Abroad Center and the Department of Biology. In addition, this study was supported by a grant (to HTS) from the Ministry of Science and Technology (MOST 108-2621-B-005-002-MY3), Executive Yuan, Taiwan. Athila Montibeller and Paula Carvalho De Castro, Geography Department (UNI), provided cartography. Access to museum specimens provided by Rafael Lemaitre and Karen J. Reed (USNM-Washington, D.C.), Karen van Dorp (RMNH-Leiden) and Marcos Tavares (ZMUSP – São Paulo).

Specimens for this research were collected under scientific permits issued by the following authorities: Florida: Environmental Protection Agency, Division of Recreation and Parks (Tallahassee) permits 04280310, 5-06-27, 12120610, and 5-06-95. Bahamas: Department of Fisheries, Ministry of Agriculture, Fisheries and Local Government (Nassau), permit MAF/FIS/17. Belize: Fisheries Department, Ministry of Agriculture and Cooperatives (Belize City) permit 00001-06 (GEN/FIS/15/04/06(03) vol.1. Jamaica: National Environmental & Planning Agency (Kingston) permit ref. no. 18/27. Puerto Rico: Departamento de Recursos Naturales y Ambientales (San Juan) permit 2008-IC-003 & US Fish and Wildlife Service, Caribbean Islands National Wildlife Refuge (Cabo Rojo), permit 41521-

090005. US Virgin Islands: Department of Planning and Natural Resources, Division of Fish and Wildlife (St. Thomas), permit STT-032-07 & US Department of the Interior National Park Service (St. John) permit VIIS-2007-SCI-0010. Barbados: ministry of Environment and Drainage (St. Michael) permit 8434/56/1 vol. iii. Curaçao: CARMABI Foundation (Piscaderabaa), permit 2012/48584. Trinidad and Tobago: Wildlife Section, Forestry Division (St. Joseph) permit Feb. 19, 2018. Guyana: Environmental Protection Agency and University of Guyana Biodiversity Center (Georgetown) permit 070618 BR010. Brazil: Instituto Brasiliero Do Meio Ambiente e Dos Recursos Naturais Revovaveis (IBAMA) permit 10BR004543/DF (CLT), MMA/ICMBio permits #18559-1, #23976-1, #29594-1 and #29594-3 to John C. McNamara (USP-RP). In addition, we wish to thank: Drs. John C. McNamara and Samuel Faria (USP-RB/CEBIMar) for facilitating collecting in Brazil; Dr. Julia Horrocks (University of West Indies-Cave Hill) for assistance on Barbados; Drs. M.J.A. Vermeij and Paul G.C. Stokkermans (CARMABI-Piscaderabaa) for support on Curaçao; Chad Thurman and Dr. Judith Gobin, Aaron Peter, and (the late) Aaron Kalloo (University West Indies- San Augustine) for help on Trinidad; Dr. Elford Liverpool and Michael Philander (The Biodiversity Institute at the University of Guyana – Georgetown) for guidance in Guyana; and HTS's laboratory for helping in molecular work. We also acknowledge two anonymous reviewers and the editor Benny K.K. Chan, who all helped improve the manuscript.

Authors' contributions: CLT conceived this study, collected and processed the samples and drafted the manuscript. REA and MJH performed the analyses of allometric and geometric morphometry, and edited the manuscript. HTS performed the molecular analysis and edited the manuscript. All authors read and approved the final manuscript.

Competing interests: The authors declare that they have no conflict of interests.

Availability of data and materials: Sequences generated in the study have been deposited in the DNA Data Bank of Japan (DDBJ) database (accession numbers in Table 1 in the manuscript).

Consent for publication: Not applicable.

Ethics approval consent to participate: Not applicable.

REFERENCES

Adams DC, Collyer A, Kalontzopoulou A. 2020. Geomorph: software for geometric morphometric analyses. R package version 3.2.1. <https://cran.r-project.org/package=geomorph>. Accessed 27 January 2020.

Albert JS, Val P, Hoorn C. 2018. The changing course of the Amazon River in the Neogene: center stage for Neotropical diversification. *Neotrop Ichthiol* **16**:e180033. doi:10.1590/1982-0224-20180033.

Behum ME, Brodie RJ, Staton JL. 2005. Distribution of juvenile *Uca pugnax* and *U. pugilator* across habitats in a South Carolina estuary, assessed by molecular techniques. *Mar Ecol Prog Ser* **288**:211–220. doi:10.3354/meps288211.

Benetti AS, Negreiros-Fransozo ML. 2004. Relative growth of *Uca burgersi* (Crustacea, Ocypodidae) from two mangroves in the southeastern Brazilian coast. *Iheringia Sér Zool* **94**:67–72. doi:10.1590/S0073-47212004000100012.

Benetti AS, Negreiros-Fransozo ML, Costa TM. 2007. Population and reproductive biology of the crab *Uca burgersi* (Crustacea: Ocypodidae) in three subtropical mangrove forests. *Rev Biol Trop* **55**:55–70.

Beinlich B, von Hagen HO. 2006. Materials for a more stable subdivision of the genus *Uca* Leach. *Zool Meded Leiden* **80**:9–32.

Borstad GA. 1982. The influence of the meandering Guiana current and Amazon River discharge on surface salinity near Barbados. *J Mar Res* **40**:421–433.

Bookstein FL. 1991. Morphometric tools for landmark data: geometry and biology. Cambridge University Press, New York, USA.

Brodie RJ, Behum ME, Monroe E, Glenn N, Staton JL. 2005. Recruitment to adult habitats following marine planktonic development in the fiddler crabs, *Uca pugilator*, *U. pugnax*, and *U. minax*. *Mar Biol* **147**:105–111. doi:10.1007/s00227-005-1557-1.

Chase FA, Hobbs HH. 1969. The freshwater and terrestrial decapod crustaceans of the West Indies with special reference to Dominica. *Bull US Natl Mus* **292**:1–258. doi:10.5479/si.03629236.292.1.

Coelho PA. 1972. Descrição preliminar de uma espécie nova de *Uca* de Pernambuco e Paraíba. In: Resumos do V Congresso Brasileiro de Zoologia. São Paulo, p. 42.

Collyer ML, Adams DC. 2018. RRPP: An R package for fitting linear models to high-dimensional data using residual randomization. *Meth Ecol Evol* **9**:1772–1779. doi:10.1111/210X.13029.

Collyer ML, Adams DC. 2020. RRPP: Linear model evaluation with randomized residuals in a permutation procedure. <https://cran.r-project.org/web/packages/RRPP>. Accessed 28 May 2020.

Collyer ML, Sekora DJ, Adams DC. 2015. A method for analysis of phenotypic change for phenotypes described by high-dimensional data. *Heredity* **115**:357–365. doi:10.1038/hdy.2014.75.

Comeau PL. 1991. Geological events influencing natural vegetation in Trinidad. *Living World (Journal of the Trinidad and Tobago Field Naturalists Club)* **1991-1992**:29–38.

Crane J. 1941. Eastern Pacific expeditions of the New York Zoological Society. XXVI. Crabs of the genus *Uca* from the west coast of Central America. *Zoologica* **26**:145–208.

Crane J. 1975. Fiddler crabs of the world (Ocypodidae: genus *Uca*). Princeton University Press, Princeton, New Jersey, 736 pp.

Endler JA. 1977. Geographic variation, speciation, and clines. Princeton University Press, Princeton, New Jersey, 246 pp.

Feest J. 1969. Morphophysiological Untersuchungen zur Ontogenese und Fortpflanzungs-biologie von *Uca annulipes* und *Uca triangularis* mit Vergleichsbefunden an *Ilyoplax gangetica*. *Forma Functio* **1**:159–225.

Floeter SR, Rocha LA, Robertson DR, Joyeux JC, Smith-Vaniz WF, Wirtz P, Edwards AJ, Barreiros JP, Ferreira CEL, Gasparini JL, Brito A, Falcón JM, Bowen BW, Bernardi G. 2008. Atlantic reef fish biogeography and evolution. *J Biogeogr* **35**:22–47. doi:10.1111/j.1365-2699.2007.01790.x.

Gibbs PE. 1974. Notes on *Uca burgersi* Holthuis (Decapoda, Ocypodidae) from Barbuda, Leeward Islands. *Crustaceana* **27**:84–91. doi:10.1163/156854074X00253.

Gibbs PE, Bryan GW. 1972. A study of strontium, magnesium, and calcium in the environment and exoskeleton of decapod crustaceans, with special reference to *Uca burgersi* on Barbuda, West Indies. *J Exp Mar Biol Ecol* **9**:97–110. doi:10.1016/0022-0981(72)90010-X.

Grantham BA, Eckert GL, Shanks AL. 2003. Dispersal potential of marine invertebrates in diverse habitats. *Ecol Appl* **13**:108–116. doi:10.1890/1051-0761(2003)013[0108:DPOMII]2.0.CO;2.

Greenspan BN. 1980. Male size and reproductive success in the communal courtship system of the fiddler crab *Uca rapax*. *Anim Beh* **28**:387–392. doi:10.1016/S0003-3472(80)80047-9.

Hagen HO von. 1970a. Verwandtschaftliche Gruppierung und Verbreitung der karibischen Winkerkrabben (Ocypodidae, Gattung *Uca*). *Zool Meded* **44**:217–235.

Hagen HO von. 1970b. Anpassungen an das spezielle Gezeitenzonen-Niveau bei Ocypodiden (Decapoda, Brachyura). *Forma Functio* **2**:361–413.

Hampton KR, Hopkins MJ, McNamara JC, Thurman CL. 2014. Intraspecific variation in carapace morphology among fiddler crabs (genus *Uca*) from the Atlantic coast of Brazil. *Aquat Biol* **20**:53–67. doi:10.3354/ab00545.

Hedgpeth JW. 1957. Classifications of marine environments. In: Hedgpeth JW (ed). Treatise on marine ecology and paleoecology, vol. 1. Ecology. *Mem Geol Soc Amer* **67**:17–28.

Hiller A, Lessios HA. 2017. Phylogeography of *Petrolisthes armatus*, an invasive species with low dispersal ability. *Sci Rep* **7**:3359. doi:10.1038/s41598-017-03410-8.

Holthuis LB. 1959. The Crustacea Decapoda of Suriname. *Zool Verhand* **44**:1–296.

Holthuis LB. 1967. On a new species of *Uca* from the West Indian region (Crustacea, Brachyura, Ocypodidae). *Zool Meded* **42**:51–54.

Hopkins MJ, Haber A, Thurman CL. 2016. Constraints on geographic variation in fiddler crabs (Ocypodidae: *Uca*) from the western Atlantic. *J Evol Biol* **29**:1553–1568. doi:10.1111/jeb.12891.

Hopkins MJ, Thurman CL. 2010. The geographic structure of morphological variation in eight species of fiddler crabs (Ocypodidae: genus *Uca*) from the eastern United States and Mexico. *Biol J Linn Soc* **100**:248–270. doi:10.1111/j.1095-8312.2010.01402.x.

Hyman OW. 1922. Adventures in the life of a fiddler crab. *Rep Smith Inst* **1920**:443–460.

Jaramillo C, Montes C, Cardona A, Silvestro D, Antonelli A, Bacon CD. 2017. Comment on “Formation of the Isthmus of Panama” by O’Dea et al. *Sci Adv* **3**:e1602321. doi:10.1126/sciadv.1602321.

Jones AR. 1980. Chela injuries in the fiddler crab, *Uca burgersi* Holthuis. *Mar Beh Physiol* **7**:47–56. doi:10.1080/10236248009386970.

Kelly RP, Palumbi SR. 2010. Genetic structure among 50 species of the northeastern Pacific rocky intertidal community. *PLoS ONE* **5**:e8594. doi:10.1371/journal.pone.0008594.

Kingsley JS. 1880. Carcinological notes, no. II. – Revision of the Gelasimi. *Proc Acad Nat Sci Philad* **1880**:135–155.

Klingenberg CP. 2011. MorphoJ: an integrated software package for geometric morphometrics. *Mol Ecol Res* **11**:353–357. doi:10.1111/j.1755-0998.2010.02924.x.

Klingenberg CP, Barluenga M, Meyer A. 2002. Shape analysis of symmetric structures: quantifying variation among individuals and asymmetry. *Evolution* **56**:1909–1920. doi:10.1111/j.0014-3820.2002.tb00117.x.

Lanfear R, Frandsen PB, Wright AM, Senfeld T, Calcott B. 2017. PartitionFinder 2: new methods for selecting partitioned models of evolution for molecular and morphological phylogenetic analyses. *Mol Biol Evol* **34**:772–773. doi:10.1093/molbev/msw260.

Latrubesse EM, Cozzuol M, da Silva-Caminha SA, Rigsby CA, Absy ML, Jaramillo C. 2010. The Late Miocene paleogeography of the Amazon Basin and the evolution of the Amazon River system. *Earth-Science Reviews* **99**:99–124. doi:10.1016/j.earscirev.2010.02.005.

Laurenzano C, Costa TM, Schubart CD. 2016. Contrasting patterns of clinal genetic diversity and potential colonization pathways in two species of Western Atlantic fiddler crabs. *PLoS ONE* **11**:e0166518. doi:10.1371/journal.pone.0166518.

Laurenzano C, Farias NE, Schubart CD. 2012. Mitochondrial genetic structure of two populations of *Uca uruguensis* fails to reveal an impact of the Rio de la Plata on gene flow. *Nauplius* **20**:15–25. doi:10.1590/S0104-64972012000100003.

Laurenzano C, Mantelatto FLM, Schubart CD. 2013. South American homogeneity versus Caribbean heterogeneity: population genetic structure of the western Atlantic fiddler crab *Uca rapax* (Brachyura, Ocypodidae). *J Exp Mar Biol Ecol* **449**:22–27. doi:10.1016/j.jembe.2013.08.007.

Leigh JW, Bryant D. 2015. PopART: Full-feature software for haplotype network construction. *Meth Ecol Evol* **6**:1110–1116. doi:10.1111/2041-210X.12410.

Levins R. 1968. Evolution in changing environments. Princeton University Press, Princeton, New Jersey, 10+120 pp.

Marcgrave G. 1648. *Historiae Rerum Naturalium Brasiliæ*. pp. 1–293 in *Historia Naturalis Brasiliæ*. Lugdun Batavorum et Amstelodami, Leyden and Amsterdam.

Melo GAS. 1996. Manual de identificação dos Brachyura (caranguejos e siris) do litoral brasileiro. Plêiade/FAPESP, São Paulo, 604 pp.

Miller DC. 1961. The feeding mechanism of fiddler crabs with ecological considerations of feeding adaptations. *Zoologica* **46**:89–101.

O'Dea A, Lessios HA, Coates AG, Eytan RI, Restrepo-Moreno SA, Cione AL, Collins LS, de Queiroz A, Farris DW, Norris RD, Stallard RF et al. 2016. Formation of the isthmus of Panama. *Sci Adv* **2**:e1600883. doi:10.1126/sciadv.1600883.

Ono Y. 1965. On the ecological distribution of ocypodid crabs in the estuary. *Mem Faculty Sc, Kyushu University E (Biol)* **4**:1–60.

R Development Core Team. 2020. R: A language and environment for statistical computing. R Foundation for Statistical Computing, Vienna, Austria. <https://www.R-project.org/>. Accessed 27 January 2020.

Rabalais NN, Cameron JN. 1983. Abbreviated development of *Uca subcylindrica* (Stimpson, 1859) (Crustacea, Decapoda, Ocypodidae) reared in the laboratory. *J Crustacean Biol* **3**:519–541. doi:10.1163/193724083X00193.

Ragionieri L, Fratini S, Vannini M, Schubart CD. 2009. Phylogenetic and morphometric differentiation reveal geographic radiation and pseudo-cryptic speciation in a mangrove crab from the Indo-West Pacific. *Mol Phylogenet Evol* **52**:825–834. doi:10.1016/j.ympev.2009.04.008.

Rasband WS. 2018. ImageJ. U.S. National Institutes of Health, Bethesda, Maryland, USA. <https://imagej.nih.gov/ij>. Accessed 01 June 2020.

Reiger PJ. 1998. Desenvolvimento larval de *Uca (Minuca) bugersi* Holthius (Crustacea, Decapoda, Ocypodidae), em laboratório. *Rev Bras Zool* **15**:727–756. doi:10.1590/S0101-81751998000300017.

Ronquist F, Huelsenbeck JP, Teslenko M, Nylander JAA. 2019. MrBayes 3.2 manual. Available at <http://mrbayes.csit.fsu.edu/manual.php>. Accessed 4 April 2020.

Ronquist F, Teslenko M, van der Mark P, Ayres DL, Darling A, Höhna S, Larget B, Liu L, Suchard MA, Huelsenbeck JP. 2012. MrBayes 3.2: efficient Bayesian phylogenetic inference and model choice across a large model space. *Syst Biol* **61**:539–542. doi:10.1093/sysbio/sys029.

Rosenberg MS. 2020. A fresh look at the biodiversity lexicon for fiddler crabs (Decapoda: Brachyura: Ocypodidae). Part 2: Biogeography. *J Crustacean Biol* **40**:364–383. doi:10.1093/jcobi/ruaa029.

Schubart CD, Diesel R, Hedges SB. 1998. Rapid evolution to terrestrial life in Jamaican crabs. *Nature* **393**:363–365. doi:10.1038/30724.

Schuh M, Diesel R. 1995. Effects of salinity, temperature, and starvation on the larval development of *Armases* (= *Sesarma*) *miersii* (Rathbun, 1897), a semiterrestrial crab with abbreviated development (Decapoda: Grapsidae). *J Crustacean Biol* **15**:205–213. doi:10.1163/193724095X00217.

Shaw RG, Mitchell-Olds T. 1993. ANOVA for unbalanced data: an overview. *Ecology* **74**:1638–1645.

Shih HT, Komai T, Liu MY. 2013. A new species of fiddler crab from the Ogasawara (Bonin) Islands, Japan, separated from the widely-distributed sister species *Uca (Paraleptuca) crassipes* (White, 1847) (Crustacea: Decapoda: Brachyura: Ocypodidae). *Zootaxa* **3746**:175–193. doi:10.11646/zootaxa.3746.1.8.

Shih HT, Ng PKL, Christy JH. 2015. *Uca (Petrucia)*, a new subgenus for the rock fiddler crab *Uca panamensis* (Stimpson, 1859) from Central America, with comments on some species of the American broad-fronted subgenera. *Zootaxa* **4034**:471–494. doi:10.11646/zootaxa.4034.3.3.

Shih HT, Ng PKL, Davie PJF, Schubart CD, Türkay M, Naderloo R, Jones DS, Liu MY. 2016. Systematics of the family Ocypodidae Rafinesque, 1815 (Crustacea: Brachyura), based on phylogenetic relationships, with a reorganization of subfamily rankings and a review of the taxonomic status of *Uca* Leach, 1814, sensu lato and its subgenera. *Raffles Bull Zool* **64**:139–175.

Shih HT, Ng PKL, Ravichandran S, Prema M. 2019. Resurrection of *Gelasimus variegatus* Heller, 1862, a fiddler crab closely related to *Austruca bengali* (Crane, 1975) and *A. triangularis* (A. Milne-Edwards, 1873) (Decapoda, Brachyura, Ocypodidae), from the Bay of Bengal, Indian Ocean. *Zool Stud* **58**:12. doi:10.6620/ZS.2019.58-12.

Shih HT, Ng PKL, Wong KJH, Chan BKK. 2012. *Gelasimus splendidus* Stimpson, 1858 (Crustacea: Brachyura: Ocypodidae), a valid species of fiddler crab from the northern South China Sea and Taiwan Strait. *Zootaxa* **3490**:30–47. doi:10.11646/zootaxa.3490.1.2.

Shih HT, Poupin J. 2020. A new fiddler crab of *Austruca* Bott, 1973, closely related to *A. perplexa* (H. Milne Edwards, 1852) (Crustacea: Brachyura: Ocypodidae), from the South Pacific islands. *Zool Stud* **59**:26. doi:10.6620/ZS.2020.59-26.

Silva IC, Mesquita N, Paula J. 2010. Lack of population structure in the fiddler crab *Uca annulipes* along an East African latitudinal gradient: genetic and morphometric evidence. *Mar Biol* **157**:1113–1126. doi:10.1007/s00227-010-1393-9.

Sokal RR, Rohlf FJ. 2012. Biometry. 4th ed. WH Freeman and Co., New York, 937 pp.

Stamatakis A. 2006. RAxML-VI-HPC: maximum likelihood-based phylogenetic analyses with thousands of taxa and mixed models. *Bioinformatics* **22**:2688–2690. doi:10.1093/bioinformatics/btl446.

Stoddart DR, Bryan GW, Gibbs PE. 1978. Inland mangroves and

water chemistry, Barbuda, West Indies. *J Nat Hist* **7**:33–46. doi:10.1080/00222937300770031.

Streets TH. 1872. Notice of some Crustacea from the island of St. Martin, W.I., collected by Dr. van Rijgersma. *Proc Acad Nat Sci Philad* **24**:131–134.

Thurman CL. 1979. Fiddler crabs of the Gulf of Mexico. Ph.D. dissertation, University of Minnesota, 290 pp.

Thurman CL. 1985. Reproductive biology and population structure of the fiddler crab *Uca subcylindrica* (Stimpson). *Biol Bull* **169**:215–229. doi:10.2307/1541399.

Thurman CL. 2002. Osmoregulation in six sympatric fiddler crabs (genus *Uca*) from the northwestern Gulf of Mexico. *Mar Ecol* **23**:269–284. doi:10.1046/j.1439-0485.2002.02785.x.

Thurman CL, Faria SC, McNamara JC. 2013. The distribution of fiddler crabs (*Uca*) along the coast of Brazil: implications for biogeography of the western Atlantic Ocean. *Mar Biodivers Rec* **6**:el-el12. doi:10.1017/S1755267212000942.

Thurman CL, Faria SC, McNamara JC. 2017. Geographical variation in osmoregulatory ability among populations of ten species of fiddler crabs from the Atlantic coast of Brazil: a macrophysiological analysis. *J Exp Mar Biol Ecol* **497**:243–253. doi:10.1016/j.jembe.2017.07.007.

Thurman CL, Hanna J, Bennett C. 2010. Ecophenotypic physiology: osmoregulation by fiddler crabs (*Uca* spp.) from the northern Caribbean in relation to ecological distribution. *Mar Freshw Beh Physiol* **43**:339–356. doi:10.1080/10236244.2010.526407.

Thurman CL, Hopkins MJ, Brase AL, Shih HT. 2018. The unusual case of the widely distributed fiddler crab *Minuca rapax* (Smith, 1870) from the western Atlantic: an exemplary polytypic species. *Invertebr Syst* **32**:1465–1490. doi:10.1071/IS18029.

van Soelen EE, Kim JH, Santos RV, Dantas EL, de Almeida FV, Pires JP, Roddez M, Damsté JSS. 2017. A 30 Ma history of the Amazon River inferred from terrigenous sediments and organic matter on the Ceará Rise. *Earth Planetary Sci Letter* **474**:40–48.

Vieira R, Pinho G, Rieger P. 2010. Juvenile development of *Uca* (*Minuca*) *burgersi* Holthuis, 1967 (Crustacea, Brachyura, Ocypodidae) in the laboratory. *Atlântica* **32**:59–70. doi:10.5088/atl.2010.32.1.59.

Wieman AC, Berendzen PB, Hampton KR, Jang J, Hopkins MJ, Jurgenson J, McNamara JC, Thurman CL. 2014. A panmictic fiddler crab from the coast of Brazil? Impact of divergent ocean currents and larval dispersal potential on genetic and morphological variation in *Uca maracoani*. *Mar Biol* **161**:173–185. doi:10.1007/s00227-013-2327-0.

Wright S. 1930. The genetical theory of natural selection: a review. *J Hered* **21**:349–356.

Zelditch ML, Swiderski DL, Sheets HD. 2012. Geometric morphometrics for biologists. 2nd ed. Academic Press, New York, 443 pp.

Supplementary materials

Fig. S1. Comparison of PCA based on symmetric component of variation (left panel; same as shown in figure 15 of main text) and PCA based on the residuals from a regression of the carapace shape data on the natural log of centroid size (right panel). Percent variation described by PC1 and PC2, and clustering based on groups regions, is similar in both. (download)

Fig. S2. Scree plot showing the percent variation explained by each principal component. The first two components explain almost 50% of the total variation. (download)

Table S1a. Specimens of *Minuca burgersi* Holthuis 1967 used for length measurements for allometric analyses. UNI = University of Northern Iowa; USNM = National Museum of Natural History (Smithsonian); ZMUSP = Zoology Museum, University of São Paulo, São Paulo, São Paulo State, Brazil. (download)

Table S1b. Specimens of *Minuca burgersi* Holthuis 1967 used for geometric morphometric analyses. Specimens are females only (see text). UNI = University of Northern Iowa; USNM = National Museum of Natural History (Smithsonian); ZMUSP = Zoology Museum, University of São Paulo, São Paulo, São Paulo State, Brazil. NA = unknown/unavailable. Meso = mesosaline; Oligo = oligosaline; eu = eusaline; hyper = hypersaline. Salinity categories based on mOsm kg⁻¹ H₂O readings from a Wescor Vapor Pressure osmometer (Thurman et al. 2013. Marine Biodiversity Records 6, el-el12). (download)

Table S2. Mann-Whitney test results for differences between centroid sizes of specimens from different regions and substrate environments. Mann-Whitney statistic is reported in the upper right corner and the associated p-value is reported up to 5 digits in the lower left corner. All p-values < 0.05 are bolded. Compare with figure 15A–C. (download)

Table S3. Full results of MANOVAs using a randomized residual permutation procedure (RRPP) and type III (marginal) sum of squares, which quantifies the effect of a particular factor adjusted for all other factors in the model (Shaw and Mitchell-Olds 1993). Effect sizes (Z) are standard deviations of observed SS-values from sampling distributions of random values found via RRPP. (download)

Dataset S1. Landmark data for geometric morphometric analysis. Data is in TPS format. This header should be removed before data is analyzed. (download)